HHS Public Access

Author manuscript

Biomaterials. Author manuscript; available in PMC 2018 June 01.

Published in final edited form as:

Biomaterials. 2017 June ; 129: 37–53. doi:10.1016/j.biomaterials.2017.02.032.

Ventricular wall biomaterial injection therapy after myocardial infarction: Advances in material design, mechanistic insight and early clinical experiences

Yang Zhu[1,2], **Yasumoto Matsumura**[1], and **William R. Wagner**[1,2,3,4,*]

[1]McGowan Institute for Regenerative Medicine, University of Pittsburgh, Pittsburgh, PA, 15219

[2]Department of Bioengineering, University of Pittsburgh, Pittsburgh, PA, 15219

[3]Department of Surgery, University of Pittsburgh, Pittsburgh, PA, 15219

[4]Department of Chemical Engineering, University of Pittsburgh, Pittsburgh, PA, 15219

Abstract

Intramyocardial biomaterial injection therapy for myocardial infarction has made significant progress since concept initiation more than 10 years ago. The interim successes and progress in the first 5 years have been extensively reviewed. During the last 5 years, two phase II clinical trials have reported their long term follow up results and many additional biomaterial candidates have reached preclinical and clinical testing. Also in recent years deeper investigations into the mechanisms behind the beneficial effects associated with biomaterial injection therapy have been pursued, and a variety of process and material parameters have been evaluated for their impact on therapeutic outcomes. This review explores the advances made in this biomaterial-centered approach to ischemic cardiomyopathy and discusses potential future research directions as this therapy seeks to positively impact patients suffering from one of the world's most common sources of mortality.

Keywords

myocardial infarction; ventricular remodeling; injectable materials; mechanical support; finite element modeling; clinical trials

Introduction

Cardiovascular diseases (CVD) are one of the leading causes of mortality worldwide. In 2012 CVD accounted for 17.5 million deaths around the world [1]. Among CVD, myocardial infarction (MI) and other types of ischemic heart diseases (IHD) are a principal

*Corresponding author. McGowan Institute for Regenerative Medicine, University of Pittsburgh, 450, Technology Drive, Pittsburgh, PA 15219, USA. Tel: +1-412-624-5327, Fax: +1-412-624-5363, wagnerwr@upmc.edu.

source of mortality [2]. The concept of intramyocardial biomaterial injection therapy was introduced and has been widely investigated during the past decade as a mechanical strategy to reduce left ventricular (LV) wall stress by mechanical load shielding, increasing LV wall thickness and decreasing the ventricle radius, thereby moderating the pathological LV remodeling process (Figure 1). In 2004, Christman et al. reported that direct injection of fibrin glue into the infarcted myocardium preserved cardiac function, decreased infarct size and increased neovasculature formation [3, 4]. Two years later, Wall et al. described the mechanical contribution of injectates in reducing LV wall stress and improving ejection fraction using finite element modeling. The injection of biomaterials into a thinned ventricular wall increases the wall thickness, thus reducing the myofiber stress, and if the injectate is properly distributed, normalizes the stress in the LV [5]. The early experimental data and the computational model laid the foundation for many subsequent investigations into cardiac wall injection therapy as a potential means for improving functional outcomes in post-MI patients.

The concept of intramyocardial biomaterial injection therapy began to capture the attention of the broader biomaterials community in the first five years after solidification of the concept, with early progress being well-summarized and highlighted by several groups in 2011 [6–8]. A variety of biomaterials including naturally-derived hydrogels, synthetic hydrogels, self-assembling peptides and microparticles have been shown to have therapeutic effects in animal models [6–8]. Among all candidate injectate materials, alginate hydrogel was the first to reach phase I clinical trials beginning in 2008 [9]. In the past five years, research and developments in the field have built momentum and significant progress has been made in virtually all aspects of the therapy, bringing this approach closer to the bedside. More biomaterials have entered pre-clinical and clinical trials. More sophisticated models for the mechanical and biological effects of biomaterial injection have been introduced. An array of designed, injectable biomaterials that incorporate specific functionalities have been reported. Optimization of parameters in the injection procedure has been stressed, and more options in minimally invasive injection procedures have been explored.

The collective effort of the community could be assembled at this point into a long-term vision for the implementation of this promising biomaterial-based intervention: (1) imaging of the patient’s heart provides data for personalized finite element model construction, emphasizing the spatial distribution of the infarct; (2) a bioactive, bulking material capable of positively influencing post-MI remodeling events is selected; (3) an injection plan with parameters guided by personalized cardiac modeling to achieve optimized mechanical and biological effects is developed; and (4) the patient undergoes the procedure to precisely deliver the biomaterial and is treated with a complementary pharmaceutical regimen to further facilitate an optimal chronic outcome. In this review, we summarize the progress in the field in the past five years that would contribute to meeting the elements that comprise this vision.

Clinical trials and large animal studies

PRESERVATION-1 clinical trial

As noted above, alginate was the first biomaterial evaluated in clinical trials. IK-5001, an alginate hydrogel (1% sodium alginate plus 0.3% calcium gluconate) developed by Leor et al. and BioLineRX (Jerusalem, Israel) was shown to have therapeutic benefit in terms of reduced LV enlargement and increased scar thickness in a preclinical (porcine) infarction/reperfusion model in 2009 and soon entered a phase I clinical trial (NCT00557531) [9, 10]. In the first-in-man study, 27 patients with moderate-to-large ST-segment-elevation MI and successful revascularization were enrolled and had IK-5001 injected within 7 d after infarction through the infarct-related coronary artery using an infusion catheter with percutaneous radial artery access [11]. In the earlier porcine model, IK-5001 was shown to diffuse through the vasculature and gel in the infarcted myocardium [10]. Six months follow up in patients showed the safety of the intracoronary hydrogel injection approach [11].

Following the phase I trial, a larger scale PRESERVATION-1 trial (NCT01226563) investigating the effectiveness of IK-5001 for prevention of ventricular remodeling and congestive heart failure was initiated [12–14]. The long-term results were recently reported with the conclusion that intracoronary injection of IK-5001 prevented neither LV remodeling compared to saline control nor the occurrence of heart failure [15]. 303 patients with large ST-elevation myocardial infarction (STEMI) were enrolled and randomized 2:1 to receive a 4 mL injection of alginate or saline in the infarct artery 2 to 5 d following MI. At 6 and 12 months, LV end-diastolic volume index increased for both groups without statistical differences. In addition, no differential improvements were observed in secondary endpoints for the hydrogel group [15]. The lack of clinical efficacy following encouraging porcine model data might be attributable to larger infarction sizes in patients, which would decrease the likelihood of delivery across the entire infarction region. It would be interesting to know how the delivered hydrogel was distributed with respect to the varied infarcts in the patient group and whether LV wall thickening was observed. Additionally, the degradation rate of the injected material was unknown. There are also conceptual concerns associated with the intracoronary delivery method. Infusion of the hydrogel precursor into the coronary arteries might be expected to be accompanied by the risks of hydrogel occluding smaller vessels and remote embolization. Such effects may be sub-clinical and obviate mechanical benefits provided by the hydrogel myocardial placement.

AUGMENT-HF clinical trial

An alternative alginate-based strategy has been pursued by Lee et al. and LoneStar Heart (Laguna Hills, USA). Unlike the IK-5001 studies, open chest surgeries were employed to directly inject alginate based Algisyl-LVR (a mixture of a Na^{+}-alginate component and a Ca^{2+}-alginate component consisting of water insoluble particles in water plus 4.6% mannitol) to infarcted canine hearts instead of with a minimally invasive approach [16]. Algisyl-LVR injection significantly increased ejection fraction (EF) and reduced LV end-diastolic and end-systolic volumes (EDV and ESV) compared to the saline injection control [16, 17]. First-in-man evaluation of the safety and feasibility of Algisyl-LVR injection therapy was initiated in 2009 (NCT00847964) [18, 19]. Six patients with ischemic (n=4) and

nonischemic (n=2) dilated cardiomyopathy in the uncontrolled pilot study received individual injections of 0.25–0.35 mL Algisyl-LVR at 10–15 locations at the LV midventricular level, halfway between the LV apex and base starting at the anteroseptal groove and ending at the posteroseptal groove. These injections were performed under direct visualization during a coronary artery bypass grafting or valve surgery and the procedure was shown to be safe and tolerable [18]. Improvements in EDV, ESV and EF were observed as early as 3 d following surgery for all patients [18]. In addition, magnetic resonance imaging (MRI) was performed to facilitate reconstruction of patient specific LV geometry in a FE model [20]. Output from the model showed an increase in the volumetric-averaged wall thickness for all patients and a 35% decrease in myofiber stress [21]. Expanding from this pilot study, the multicenter AUGMENT-HF trial (NCT01311791) enrolled 78 patients with advanced heart failure (LVEF≤35%, peak VO_2 of 9.0–14.5 mL/min/kg), randomizing them to an experimental group receiving Algisyl-LVR injections in addition to standard medical therapy or to a control group receiving standard medical therapy alone [22]. Over the 12 month follow up, mean peak VO_2 and mean 6 min walk distance gradually increased in patients injected with Algisyl-LVR while these parameters worsened in the control group [22]. Despite favorable trends in EF shortly after injection [18], LV end-diastolic diameter (EDD), LV end-systolic diameter (ESD), and LV mass were observed over time for the Algisyl-LVR group, none of these parameters varied significantly between the treatment groups [22].

Apart from the positive outcomes of the AUGMENT-HF trial, the delivery method (sternotomy or thoracotomy) excludes patients receiving exclusively percutaneous coronary interventions (PCI). On the other hand, the compression modulus of Algisyl-LVR is 3–5 kPa [21], which is less than normal myocardium and stiffer fibrotic tissue, leaving considerable room for improvements in creating a mechanical shielding effect. In addition, although the relatively simple composition of the alginate hydrogels is attractive from a regulatory perspective, the bioactivity of such hydrogels is limited, suggesting another direction for improving therapeutic outcomes.

Phase I clinical trial of extracellular matrix hydrogel (VentriGel)

A hydrogel (VentriGel) derived from decellularized porcine myocardial tissue has been developed by Christman et al. and Ventrix, Inc (San Diego, CA) and is recruiting patients for phase I clinical trial (NCT02305602) [23–25]. The uncontrolled study will evaluate the safety and feasibility of trans-endocardially delivered VentriGel in patients with LVEF of 25–45% secondary to MI. Primary endpoints will be serious adverse events in the 6 months after injection, and secondary endpoints will be efficacy indicators including ESV, EDV, EF and scar mass [24]. Unlike the aforementioned PRESERVATION-1 and AUGMENT-HF trials, patients will receive VentriGel injection via a MyoStar catheter and NOGA® mapping will guide injections that will occur 60 d to 3 yr after MI. This population will thus represent infarcts that are in the chronic stage and will be the first clinical trial to evaluate the efficacy of injection therapy in this later period. The use of a gel derived from decellularized cardiac tissue provides a means to deliver structural and functional molecules secreted by the resident cells of a specific tissue source and preserved in the subsequent processing steps [26]. These types of materials have been derived from numerous tissue sources and shown to

provide therapeutic effects in a broad variety of tissue engineering and regenerative medicine applications [27], [28]. VentriGel injection into porcine myocardial infarcts has been associated with improvements in cardiac function, ventricular volumes, global wall motion scores, and blood vessel formation, while not exhibiting damage to peripheral tissues, nor disrupting cardiac rhythm [29, 30]. The safety and efficacy of the endomyocardial delivery method using arterial access were also confirmed in this model.

Large animal studies

During the last 5 years, more materials have been evaluated in preclinical trials. Aside from the aforementioned alginate based hydrogels and ECM hydrogel, hyaluronic acid (HA) based materials and calcium hydroxyapatite microspheres are the most extensively studied. Polypeptide and synthetic hydrogels have enriched the variety of biomaterials that have reached the stage of large animal studies. A summary of recent large animal studies are presented in Table 1. The majority of these studies demonstrated functional improvements at their endpoints. Some new challenges that were not encountered in small animal models, but that are more relevant to clinical conditions, were experienced. Smaller infarctions were made in the larger animals since larger infarctions were less tolerable, as is the case in humans. Across different studies, significantly more injections were made in order to cover the infarction area as the absolute infarction area and muscle volume were far greater than for rodent models. Thus the design of injection distribution was also a new issue (that will be discussed in a subsequent section). Although the potential injury from relatively large-volume injections has not been illustrated in depth, relative smaller volumes were unanimously chosen by all of the large animal studies, meaning that more injections were needed to achieve similar volume fractions of injectate in the large animal model. Last but not least, the feasibility of minimally invasive delivery methods could be demonstrated in large animals, which has led to their application in the aforementioned clinical trials.[17, 29–42]

The porcine model is one of the more frequently utilized large animal models and is attractive in that the coronary artery system is very similar to that of humans [43, 44], with the right-side dominant manner in which the blood is supplied to the coronary artery system. Also, the conduction system is similar to 90% of the human population [43]. Since there is little collateral blood supply, a distinct infarct is easier to create, whereas in other animal models such as dogs the collateral circulation makes such infarcts difficult to achieve [44]. However, there are several differences between the porcine model and the clinical situation that need to be considered when analyzing the results in large animal studies. First, the infarctions are usually created with ligations or intra-arterial occlusions in young, otherwise healthy animals, lacking the underlying chronic cardiovascular disease (e.g. arteriosclerosis and hypertension) and other co-morbidities present in the target clinical population. Secondly, the majority of the reported large animal studies did not involve a reperfusion or revascularization process (Table 1). The priority for MI patients is to reestablish the blood supply to the endangered myocardium. Skipping the reperfusion process not only skips the observation period afterwards, more importantly it excludes the reperfusion injury from the animal models, whereas reperfusion injury is a substantial complicating factor defining the extent of an infarct and efficacy of later interventions [45–47]. Finally, over 60% of the

studies listed in Table 1 delivered the hydrogel within 60 min after infarct creation. This time frame is not realistic for the majority of patients suffering MI and at risk for ischemic cardiomyopathy.

Mechanisms of biomaterial injection therapy and influence of injection parameters

Initiated by the mechanical analysis of Wall et al., the discussion of the mechanical effect of ventricular wall biomaterial injection has been a focus of mechanistic studies [5, 48]. In the last 5 years, substantial progress has been made in the areas of personalized mechanical analysis supported by advanced imaging techniques, understanding the influence of material distribution and modulus on the mechanical properties of the LV, and additional biological effects from injected biomaterials beyond wall thickening and stiffening.

Computational mechanical simulation based on imaging derived models

Due to the complexities and limitations in collecting real-time, in vivo measurements, computational modeling has become a dominant tool for characterizing the mechanical impact of hydrogel injection. In a study combining experimentation and modeling, Kichula et al. validated the LV stiffening and fiber stress relieving effect predicted by FE models with biaxial testing [49]. Early computational efforts employed simplified cardiac geometries better suited for addressing the general phenomena driving injection therapy [48]. More recently, imaging techniques, particularly MRI, have facilitated the development of case-specific construction of FE models with increasing detail.

Wenk et al. generated the contour points for an FE model from real-time 3D echocardiography of sheep with anteroapical infarcts at the end of diastole and systole [50]. Dorsey et al. developed FE models specific to experimental pigs in a 12 w study and achieved serial, non-invasive estimation of infarct material properties [33]. Global LV structure and function were assessed by cine MRI, and infarct expansion was visualized by late-gadolinium enhancement (LGE) MRI. Tissue strain was assessed from passive wall motion given by epicardial tagging, and was used to calculate the physical properties of infarcted myocardium through an FE model [33].

With patient-specific MRI data from the AUGMENT-HF trial, Lee et al. described a protocol to build an FE model of the LV which captured the contraction-dilation movements and ED and ES pressures [20]. The contour was derived by digitizing the endocardial and epicardial surfaces, as shown in Figure 2. Material properties as model parameters were adjusted to match the computed EDV and ESV with the imaged volumes [20]. The fiber stress calculated from the model was shown to decrease as a result of hydrogel injection, accompanied by improved cardiac function, increased wall thickness and reversed remodeling (Figure 2) [20, 21]. In this study, predefined myofiber directions were assigned to the model to generally mimic cardiac anatomy. Recognizing the significant and sensitive influence of myofiber orientation on LV mechanics, a diffusion tensor magnetic resonance imaging (DTMRI) based approach was recently described to derive patient-specific myofiber orientation. Toussaint et al. acquired 2D diffusion tensor images in healthy

volunteers and proposed a dense approximation scheme of the complete 3D cardiac fiber architecture of the LV that was validated using ex vivo hearts [51]. This method is expected to capture local fiber disarray for individual patient infarct regions, which could facilitate the incorporation of the first patient-specific fiber orientation into the patient's in silico reconstructed LV geometry [48, 51].

Influence of biomaterial properties and injection parameters

In addition to acquiring accurate, patient-specific geometric and mechanical cardiac representations, studying the influence of biomaterial properties and injection parameters has been another important research direction to understand the mechanical effects of biomaterial injection. Based on the aforementioned patient-specific modeling study in the AUGMENT-HF trial which demonstrated the stress-relieving effect of hydrogel injection, Lee et al. analyzed potential residual strains and stresses introduced by the same treatment with a modified patient-specific computational model [52]. The simulation showed that the residual stress can lead to more heterogeneous regional myofiber stress and strain fields. Hydrogel injection lowered the stress and stretch in the lateral regions between the injection sites, while above and below the injection site the stress and stretch were increased [52]. This result also highlighted the regional complexity that can result from biomaterial injection beyond broadly described wall thickening and stiffening.

As biomaterial viscosity, gelation mechanisms, injection locations and LV myocardium conditions vary, the distribution of an injected biomaterial may differ markedly, resulting in distinct geometric and mechanical impact on the LV. For example, computational models in a canine infarction model showed that a striated hydrogel distribution was superior to a bulk distribution in terms of reducing wall stress, while the latter was more effective when the hydrogel was delivered later in the remodeling period to the dilated LV wall, where the local tissue would be stiffer and thinner [53]. Similarly in a human MRI derived model, a striated distribution exhibited a greater impact on wall stress and strain at the acute stage while a bulk distribution benefited the fibrotic stage more (Figure 3A,B) [54]. In a rat in vivo model, bulk distribution of a degradable PEG hydrogel was achieved as injected 1 w after MI, which showed significant improvements in scar thickness and cardiac functions compared to the striated distribution associated with injection immediately after MI (Figure 3C,D) [55]. However, since the hydrogel was delivered at different time points, the differences in functional outcomes cannot be attributed to intramyocardial distribution of the biomaterial alone, as is discussed below.

In addition to biomaterial distribution, the total volume of biomaterial injected affects the observed mechanical changes. Computational simulations by Wall et al. showed that a biomaterial injection corresponding to a 4.5% increase in LV wall volume reduced post-MI border zone fiber stresses and positively affected EF and global function, whereas smaller volume changes (0.5% to 1.5%) did not have such an effect [5]. In a sheep model Dixon et al. found that 1.3 mL microparticle injection did not favorably impact the post-MI remodeling process, in contrast with functional improvements observed in animals receiving 2.6 mL injections [39]. As the peak LV mass for adult males and females are 200 and 145 g respectively, and decrease with age, [56, 57] the minimum effective injection volume can be

predicted to be 5–8 mL based on the model of Wall et al [5]. Therefore, the less-than-expected effects of the PRESERVATION-1 trial (injection volume = 4 mL) and AUGMENT-HF trial (injection volume <5 mL) may potentially be attributed to inadequate injection volumes. Wise et al. evaluated the influence of hydrogel injectate volumes in an FE model of rat infarcts. The results showed that the therapeutic effects of hydrogel injection, including ventricular function and wall mechanics, increases with injection volume, but this benefit is limited or decreases at higher levels, indicating the existence of a threshold or an optimal volume [58].

In addition to material choice and injection parameters such as material distribution and volume, the timing of biomaterial delivery post-MI is a critical factor, as well. Key events including myocyte apoptosis and necrosis, acute and chronic inflammation, and fibrosis in LV remodeling occur consecutively after MI, continuously reshaping the local mechanical and biological environment [59]. Therefore the influence of injected biomaterials is superimposed on highly dynamic remodeling processes and would be expected to exert different effects based upon when the intervention is applied. A positive functional effect from alginate hydrogel injection on LV remodeling in rats has been observed in both recent and older infarcts (1 and 8 w post-MI), as a general model of patients at differing stages of remodeling following MI [60]. Kadner et al. compared the efficacies of injecting a matrix metalloproteinase (MMP)-sensitive PEG hydrogel immediately or 1 w after MI in rats. Immediate delivery resulted in the diffusion of hydrogel through the myocardium, while delayed injections resulted in the formation of a bulk hydrogel pocket. Also of note, the hydrogel degraded much faster when delivered immediately after MI compared to 1 w post-MI, another result of the differing physical and biological LV wall milieu. These differences are intertwined with the findings that beneficial functional effects were observed only in the 1 w group [55]. Yoshizumi et al. tested three injection time points in a rat model: immediately after MI, 3 d post-MI, and 2 w post-MI corresponding to the beginnings of the necrotic, fibrotic and chronic remodeling phases. The best therapeutic outcomes were found when the polyNIPAAm-based hydrogel (NIPAAm: N-Isopropylacrylamide) was injected 3 d after MI and this outcome was related to population fluctuations in neutrophil and macrophage infiltration and inflammatory signals [61]. This study also implied the existence of an optimal window for biomaterial injection.

Biological response induced by injection therapy

Recent research reports have also focused on the biological response to biomaterial injection therapy. As the injected biomaterials alter the local mechanical environment for the preexisting and post-MI recruited cells, these cells translate the mechanical inputs to downstream biological signals. In addition, the injected biomaterials and their degradation products could, for instance, shift the pH and ion balance in the niche, and influence the inflammatory, fibrotic and foreign body responses. Some biomaterials with inherent bioactivity such as the ECM-derived hydrogels, may induce desirable post-injection therapeutic outcomes. Histological evidence of increased vascularization, reduced inflammation and mitigated scar formation due to biomaterial injection has been extensively reported across studies involving various types of biomaterials [60–65]. For instance, Zhao et al. showed that functional improvements following post-MI injection of a hydrogel

derived from small intestine ECM were associated with recruitment of c-kit-positive cells, myofibroblasts, and macrophages [66]. Chen et al. reported murine heart regeneration with evidence of cardiomyocyte and cardiac precursor cell proliferation induced by the injection of decellularized zebrafish cardiac ECM [67].

In an ovine MI model, Dixon et al. examined the influence of calcium hydroxyapatite (CHAM) injection on matrix synthetic and proteolytic pathways. Downregulation of MMP-13, MMP-7 and collagen was found in the CHAM injection group compared with MI only controls, suggesting that the favorable therapeutic effect with CHAM injection was partly due to alteration of MMP/TIMP (tissue inhibitors of MMPs) profiles [39]. Wassenaar et al. attempted to better understand the effects of ECM-derived hydrogel injection treatment on local cellular response. Over 2,000 genes were analyzed with a whole transcriptome microarray 3 d and 1 w after injection to identify potential pathways linked to the previously reported beneficial outcomes [30, 68]. Principal component analysis and pathway analysis showed that alterations in pathways associated with the inflammatory response (Figure 4), cardiomyocyte apoptosis, infarct neovascularization, cardiac hypertrophy and fibrosis, metabolic enzyme expression, cardiac transcription factor expression, and progenitor cell recruitment all may have contributed to cardiac functional improvement [68]. Suarez et al. explored the influence of biomaterial injection on action potential propagation across the heart [69]. PEG hydrogels were injected into healthy and infarcted rat hearts as a model material and were found to delay action potential propagation across the LV epicardium compared to saline injection and sham controls [69]. In addition, it was found that a highly diffused hydrogel does not alter action potential propagation, while a hydrogel that did not spread as extensively would reduce gap junction densities and may create a substrate for arrhythmias [69].

Despite the aforementioned progress, the links between the mechanical effects of biomaterial injection and histological and functional improvements are still weak and incomplete. The key components corresponding to each bioactive injectate are yet to be identified. It is well known that the renin-angiotensin system (RAS) is an essential regulator of cardiac functions, and that high mechanical load induces elevation of angiotensin II (Ang II), a factor that plays an important role in ventricular remodeling (Figure 5) [59, 70–72]. Pathologically high Ang II levels lead to adverse post-MI responses including high oxidative stress, inflammation and fibrosis, therefore administration of Ang II blocker or angiotensin converting enzyme inhibitor has shown beneficial effects in MI treatment [73, 74]. Thus the RAS and Ang II could be the key to establishing a link between the mechanical effect of biomaterial injection and related pathological responses. For ECM-derived biomaterials, identifying key components could facilitate the enhancement of corresponding benefits. For example, Okada et al. evaluated 2 forms of porcine-derived small intestinal submucosa (SIS) hydrogels as injectates for MI treatment and found that the level of basic fibroblast growth factor may partly explain the differential efficacies [75]. Chen et al. found a significantly higher level of neuregulin-1 in ECM derived from regenerating zebrafish myocardium compared to adult mouse cardiac ECM, and ErbB2 signaling played an important role in induction of a regenerative effect in an acute mouse MI model [67].

Prediction of therapeutic outcomes

Progress in mechanistic studies of biomaterial injection therapy may facilitate outcome prediction and personalized designs for future patients. Although the problem is complex, computational models might serve as valuable indicators in clinical planning. Modeling would start with a detailed description of the LV geometry, and possibly regional cell metabolism and systemic levels of humoral factors known to influence the remodeling outcome (e.g. Ang II). Patient-specific myofiber orientation could be incorporated into the geometric model and would influence the mechanical model and gel diffusion. This information would depend upon advancing DTMRI technology. Sirry et al. developed an imaging-based method to construct detailed cardiac architectures of the heart after biomaterial injection by combining the digitized distribution of injected biomaterial in a representative infarcted heart with the geometry of the heart being treated [76]. Histological sections of infarcted rat hearts that were injected with PEG hydrogel were used to reconstruct the hydrogel distribution first. Subsequently, cardiac MRI data of a second heart were collected to create an end-diastolic biventricular geometry and further adjusted to overlay the hydrogel geometry, which generated the predicted computational model of the cardiac wall post-injection [76]. Finally, the model might depict the long-term mechanical and biological effects of the injection therapy by incorporating predicted outcomes from local inflammation, fibrosis and biomaterial degradation on the local geometry and mechanics to influence cardiac output. For instance, to predict scar structure following MI, Rouillard et al. coupled an agent-based model that predicts the integration of physiological cues by fibroblasts to a finite-element model that simulates local mechanics [77]. As the local mechanics at any given time point were predicted based on collagen fiber structure, which can be linked to fibroblast activity, the coupled model captured the dynamic interplay between scar deformation, mechanical loading, and scar material properties [77].

New strategies in material design

Biomaterial injection therapy for the cardiac wall continues to focus broadly on two putative modes of action, mechanical and biological. Material design to enhance or add to these properties has been the subject of extensive investigation, together with strategies to create materials that open new possibilities for delivery and retention in the infarcted tissue. One driving force behind the development of such materials has been the debate as to whether mechanical effects from biomaterial injection alone are sufficient for cardiac functional benefit [15, 32, 78]. Rane et al. injected bio-inert PEG in rat MI model, but the polymer treated group did not show functional benefit compared to the saline control [78]. In a separate study using a slightly different PEG hydrogel, Dobner et al. achieved temporary mitigation of LV remodeling, but with the absence of long term geometrical or functional improvements [79]. Although the lack of observed beneficial effect may be due to a variety of reasons, e.g. non-degradability of injectates, the design of biomaterials with specific mechanical and biological functionalities, and coordinated interaction with the post-MI remodeling process, is of growing interest.

Electroactive materials

Synchronized electrical signal transduction is essential for normal myocardial contraction. As noted previously, an injected hydrogel with minimal interstitial spreading may delay LV activation upon injection and reduce gap junction density, possibly resulting in an arrhythmia [69]. Therefore, efforts have been made to fabricate conductive injectable biomaterials for MI treatment. Mihic et al. grafted polypyrrole (PPy) to nonconductive chitosan to create a semiconductive PPy-chitosan hydrogel [80]. In a rat MI model, PPy-chitosan injection improved conduction as indicated by a decreased QRS interval and increased transverse activation velocity compared to saline or chitosan controls. The material conductivity also contributed to improved cardiac function in comparison with the chitosan group, in addition to the therapeutic effect from chitosan injection [80]. Cui et al. synthesized a conductive polyNIPAAm-based biodegradable thermoresponsive hydrogel by covalently attaching electroactive tetraaniline (TA) to a sidechain of the copolymer (Figure 6A) [81]. Under pulsed electrical stimulation this hydrogel supported cell proliferation and differentiation of H9c2 cells, especially when doped with HCl, and the TA component endowed antioxidant activity to the hydrogel [81]. However, this study did not report cardiac injection data. Baei et al. incorporated gold nanoparticles into chitosan to generate electroactive hydrogels (Figure 6B) [82], which represents a facile strategy of adding conductive particulates (e.g. metallic particles, carbon nanotubes, graphene nanosheets) to nonconductive hydrogel substrates to create conductive injectable biomaterials. For example, Annabi et al. introduced a highly elastic and conductive hydrogel based on recombinant human tropoelastin and graphene oxide nanoparticles. The composite hydrogel electrically connected explanted abdominal muscles in vitro and supported the growth and maturation of cardiomyocytes [83].

Injectable bioactive materials

A separate focus for adding functionality to injectable biomaterials has been the covalent attachment of bioactive cues or moieties capable of binding bioactive signaling molecules. Reis et al. conjugated a chitosan-collagen hydrogel with QHREDGS, an angiopoietin-1-derived peptide that supports cardiomyocyte survival and binds to integrins [84]. The peptide functionalized hydrogel was retained in the myocardium for more than 2 w and increased the proportion of cardiac troponin-T^+ cells (cardiomyocytes) compared to controls. Cardiac function and scar formation were improved compared with peptide-free hydrogel and MI only controls [84]. Lin et al. injected platelet-derived growth factor-BB (PDGF-BB) binding peptide nanofibers 1 month after infarction in a porcine model [41]. Three months after injection, myofibroblast replenishment was promoted, LV remodeling was positively influenced and cardiac diastolic function was improved [41]. A glutathione containing chitosan hydrogel was developed by Li et al., which showed antioxidant properties and corresponding cardiomyocyte protection against reactive oxygen species in vitro [85]. In vivo influence on cardiac functions awaits evaluation.

Rocca et al. have fabricated a gelatinized alginate hydrogel with uniform capillary-like channels and directly injected this hydrogel into the antero-septal wall at the infarct border zone [86]. Cardiac function was improved compared to saline injection control in a rat injection trial. In addition, the injected hydrogel was vascularized and populated by $CD68^+$

macrophages. These macrophages largely showed an M2-like phenotype as marked by CD206 expression, suggesting a constructive remodeling response [86]. Similar local tissue responses have been observed in disease models treated with decellularized matrix materials [26, 28, 87]. Along these lines, Johnson et al. have extracted hydrogel material from human myocardial matrix, which has similar in vitro physical properties to porcine myocardial derived hydrogels. In vivo therapeutic effects are yet to be determined [88]. Chen et al. decellularized regenerating zebrafish myocardium, which enabled regeneration of adult mouse cardiac tissue and functional recovery after injection in an acute MI model [67].

New in situ crosslinking strategies

Despite the high targeting efficacy achieved in the aforementioned studies and the attractiveness of a peripheral injection approach, the mechanical effect for such approaches tends to be weakened as the particles do not crosslink to form a more mechanically robust network [89–92]. However, in situ crosslinking in the myocardium might remedy this shortcoming. Nguyen et al. designed nanoparticles which passively accumulate in the infarcted area through the enhanced permeability and retention effect and respond to local enzymatic stimuli (MMPs), resulting in the decomposition of the nanoparticles and subsequent transformation into a network embedded in the myocardium, as shown in Figure 7 [93]. Two days after tail vein injection in a rat MI model, the responsive nanoparticles could be found in the infarct and border zone, but not the remote myocardium. The polymer was observed 28 d after injection, demonstrating long-term LV retention [93]. The crosslinked network could theoretically lower local mechanical stress, especially during ventricular dilation. However, in theory, responsive nanoparticles can only migrate into the existing extracellular space, which may limit the extent of the wall thickening effect. In contrast, injected biomaterials are propelled by the pressure in the syringe or catheter, leading to the expansion of the injection space, and possibly greater ventricular wall thickening. Despite the potentially limited physical thickening effect associated with this delivery approach, wall stress reduction can still be enhanced with the implementation of crosslinking mechanisms that stiffen the delivered material network.

Novel in situ gelation mechanisms have been adopted in many recent hydrogel designs to create mechanically stronger, diffused gelation networks at injection sites. Bastings et al. developed supramolecular ureido-pyrimidinone (UPy) modified PEG hydrogels which remained a low viscosity fluid at high pH (>8.5), but underwent sol-gel transition in the infarcted myocardium with its lower pH [40]. The pH responsiveness allowed catheter-based delivery in a porcine MI model that showed the safety of the delivery method [40]. Xu et al. developed a two component system consisting of thiolated collagen (Col-SH) and oligo(acryloyl carbonate)-b-poly(ethylene glycol)-b-oligo(acryloyl carbonate) (OAC-PEG-OAC) copolymers, which gels under physiological conditions via Michael-type addition [94]. The mechanical strength, gelation time and degradation rate can be tuned by the concentration and ratio of the two components, and degree of substitution for Col-SH. The hydrogel significantly improved cardiac function and reduced infarct size in a 28 d study employing a rat infarction model [94]. Bai et al. employed an aldehyde-amine reaction to crosslink oxidized alginate with collagen upon intramyocardial injection. Compared with a calcium-crosslinked alginate hydrogel, the crosslinked alginate/collagen hydrogel reduced

matrix metalloprotease activity and achieved a smaller expansion index [95]. Rodell et al. developed an alternative to photo-crosslinkable methacrylated HA hydrogels by substituting the photo-crosslinking with a host-guest assembly method (Figure 8) [96]. Adamantine and β-cyclodextrin were attached to HA respectively to form a two-component hydrogel system. The host-guest interaction renders the hydrogel shear-thinning and provides injectability while maintaining stability [96]. This hydrogel was shown to improve cardiac function in a rat MI model [97]. Additionally, Rodell et al. combined thiol-ene Michael addition with the host-guest assembled hydrogel to further increase hydrogel modulus and stability. The dual-crosslinked hydrogel exhibited an enhanced therapeutic outcome compared with hydrogel crosslinked by sole host-guest assembly in both rat and ovine model [35, 98]. The shear-thinning property also facilitated percutaneous delivery via endocardial injection under fluoroscopic and echocardiographic guidance in sheep [35].

Controlling injectate modulus and degradation rate

To achieve a more comprehensive and deeper understanding of the influence of specific biomaterial parameters on injection therapy, there has been an increasing focus on modulating injectate properties such as modulus and degradation rate, while maintaining the same material platform. Ren et al. synthesized polyNIPAAm-based hydrogels with fast and slow degradation by copolymerization with differing ratios of dextran-PCL containing macromonomer. A rat MI model showed that myocardial contractility was greater with the slower degrading hydrogel (50% weight loss in 30 d) compared with the faster degrading version (50% weight loss in 3 d) [99]. Based on another previously proven effective hydrogel, Zhu et al. introduced an auto-catalysis strategy to modulate the degradation rate of polyNIPAAm-based thermally responsive hydrogels which allowed the hydrogel to decompose on a tunable time scale from days to months [100, 101]. Varying the crosslinking density and hydrolytic stability of crosslinkers, Tous et al. fabricated two degradable HA hydrogels (50% weight loss in ~20 and 60 d) and two hydrolytically stable hydrogels with different modulus (low: ~7 kPa; high: ~35−40 kPa). Results from an ovine MI model indicated that all hydrogels resulted in better cardiac output compared to the MI control group, and the stiffer, stable hydrogels were more effective in limiting expansion of LV volume [34]. The typical moduli range for investigated injectable hydrogels varies from 1 Pa to 100 kPa [62, 88, 102], thus the conclusion derived above was comparing materials on the relatively stiff end of this range and may have limited applicability to softer materials. At the lower end of the stiffness range, the moduli of extracellular matrix based hydrogels have been increased by crosslinking, yet the influence on injection therapy is yet to be determined [103, 104].

Injectate distribution and topography

Once injected, the distribution assumed by the biomaterial may also be an important factor in achieving a maximal therapeutic effect. This is illustrated by computational models [53, 54], as discussed above. In concert with imaging, injection pattern planning may be pursued prior to surgery, but material design will influence the spread of the injectate once infused into the cardiac wall. Direct injection of microparticles into the cardiac wall leads to injectate pocket formation regardless of particle geometry (microrods, microcube, microspheres) whereas nanoparticles quickly diffuse through the myocardium [37, 105,

106]. For hydrogel materials, viscosity and gelation time are the major determining factors of distribution. For example, less viscous, slow gelling ECM hydrogels diffuse to distal tissue while more viscous, rapid gelling alginate and HA hydrogels tend to form hydrogel "islands" upon injection [17, 30, 34]. Zhu et al. increased the hydrophilicity of a polyNIPAAm-based hydrogel by incorporating a higher percentage of N-vinylpyrrolidone monomer in the polymer backbone, obtaining a low viscosity, slower gelling version. While the relatively hydrophobic hydrogel formed isolated masses in the myocardium, higher hydrophilicity allowed the hydrogel to diffuse through the tissue before gelling [107].

Currently, the major injectate topographies are aggregated microparticles, discrete hydrogel deposits and diffuse hydrogel networks. However, there are only a few studies (including the aforementioned study on the influence of injectate distribution [55]) directly comparing these geometries on the same material platform. Pinney et al. found that injected microcubes and microrods induced differing therapeutic effects in a rat infarction/reperfusion model [105], which showed the influence of injectate microstructure in treating MI. On the other hand, recent advances have introduced methods of fabricating injectable porous materials, especially injectable porous hydrogels [108–110]. As porous structures have been proved capable of positively affecting biological responses including cell infiltration, neovascularization and foreign body responses in various medical applications [108, 111], it might be expected that injectable porous materials could further improve therapeutic outcomes.

Visualization of injected biomaterials

Visualization of injected biomaterial in vivo could provide important information on hydrogel distribution and degradation, which could be useful for evaluating the relationship between injection therapy delivery strategy and the efficacy of the treatment. In small animal models visualization has been achieved by quantum dots for fluorescent imaging, radionuclide imaging and computed tomographic (CT) imaging [106, 112, 113]. In addition, optoacoustic imaging could be a potential tool to not only follow the location and amount of injectate in vivo, but also to provide a noninvasive method to measure the mechanical strength of the injected material and the myocardium [114, 115]. However, imaging depth and scanning area are relatively limited for fluorescent and optoacoustic imaging [116] and repeated radiation exposure by CT might be a concern for patients. The injectates would also need to be radio-opaque or otherwise labeled for these methods. For extracting patient cardiac geometric and functional information, and establishing case-specific computational models, MRI has become a leading imaging tool in preclinical studies [49]. Dorsey et al. covalently attached an arginine-based peptide to HA hydrogel, which resulted in a 2-fold enhancement in signal strength in chemical exchange saturation transfer MRI and allowed discrimination between different hydrogel materials and surrounding tissue based on their chemistry [117]. Combining material design with the versatility of MRI techniques can be foreseen to provide attractive levels of patient-specific, real-time visualization for cardiac injection therapy.

Injection methods

As discussed above, injection parameters including volume, distribution and timing may have great impact on the outcome of injection therapy. In addition, the mechanisms and time course for an injectate to “set up” in situ varies with injectate chemistry. Chemical crosslinking, shear-thinning polymers, temperature-driven phase change, pH or ionically driven gelation, have all been employed, while other materials are not designed to undergo any substantial change in mechanical properties [6, 40, 96]. Depending on whether injection occurs in an open surgical field, through a minimally invasive, remote approach, or intravascularly, concerns and constraints on the hydrogel design arise. Risks to the patient associated with the errant delivery of a gelling material into the blood stream (embolic damage) are a clear concern. Further, the ease and precision of the delivery mechanism will have direct impact on the adoption and efficacy of the therapy. Injection methods that can leverage current surgical and minimally-invasive technologies may lower the translational barrier and be adopted with a lower complication risk.

Direct epicardial injection

Direct epicardial injection of biomaterial into the LV wall through sternotomy or thoracotomy is the easiest method to control and is theoretically compatible with all types of injectates. As the surgical field is exposed to the clinician, pre-determined injection locations and volumes can be easily achieved and improvised. The precision of direct injection can hardly be challenged by other methods. Another derivative advantage is that the delivery pathway and time spent by a biomaterial in this pathway is minimized. This parameter may be important with materials that rely upon phase change or chemical reaction that may be initiated during the delivery process.

The AUGMENT-HF trial has proven the safety and feasibility of direct cardiac wall injections in MI patients receiving CABG. CorMatrix (Roswell, GA) has developed a porcine ECM delivery system composed of a multi-needle syringe assembly, an automated injection controller, and a portable ultrasound tissue depth measurement system, as shown in Figure 9. Slaughter et al.demonstrated the feasibility of gas propelled injections in a bovine model of chronic ischemic cardiomyopathy, as well as the ability to control injection volume (0.1–1.0 mL) and penetration depth (3–5 mm) under regulated injection pressure into the target region [118]. However, due to the open-chest requirement for direct injection approaches, the patient population suitable for such an approach is limited. In the AUGMENT-HF trial, patients received injection therapy immediately following CABG surgery, thus a separate sternotomy or thoracotomy was not required. For patients undergoing percutaneous revascularization procedures, a subsequent open-chest procedure would not be an attractive option. A related constraint of an open chest approach is that the injection therapy would likely need to be performed at the time of CABG and could not be optimized to some earlier or later time point.

Minimally invasive approaches

For patients not receiving CABG or where injection therapy could not be performed in conjunction with this surgery, minimally invasive delivery approaches are highly favored. A

variety of systems have been developed in recent years to facilitate fluid or cell delivery to the cardiac wall [119–121]. These technologies provide the framework to achieve minimally invasive biomaterial injection therapy. Ota et al. developed a novel miniature robotic device (HeartLander) that can navigate on the surface of the beating heart and make guided injections [122]. Zhu et al. delivered a polyNIPAAm-based biodegradable thermally responsive hydrogel into the LV wall of a live porcine heart using HeartLander. Through a small subxiphoid incision, the HeartLander crawler approached the LV, went under the pericardium and used an applied vacuum to anchor on the epicardium (Figure 10A, B). Guided by a real-time tracking system, the crawler moved on the beating heart through "release-re-position-anchor" cycles (Figure 10C) and could navigate to the planned injection sites. Cooled by a fluid sheath around the catheter, the hydrogel was kept in the liquid phase prior to the injections. Four injections in the planned square layout were made, as shown by photoacoustic imaging (Figure 10D, E) [107]. The HeartLander delivery system was considered suitable for a wide variety of injectable biomaterials.

As described above, PCI procedures including intra-arterial infusion and endocardial injections have been employed in clinical and preclinical trials [15, 29, 30, 35]. PCI is widely employed in coronary artery stent placement and other therapies, thus the technical challenges for clinicians mastering this approach would be minimized. A potential drawback is the theoretical risk of biomaterial regurgitation or leakage into the vascular system, causing remote embolization. For intra-arterial infusion, where the presumption is that the material will cross only into the infarcted region and gel there, there is also concern for undesired gelling to occur in non-targeted tissues. For these two administration routes biomaterials with fast solidification kinetics would appear to be a greater risk of forming a mechanically stable embolus. On the other hand, as the intravascular injection route requires long catheters to run through the vasculature, biomaterials that employ thermally-triggered gelling are less compatible due to concerns of material solidification in the catheter and occlusion of the lumen. For injectable biomaterials that actively or passively target the infarcted myocardium, intravenous injections have been employed in animal models [89, 90, 92]. Intravenous injection is the least invasive delivery method, although there are considerable limits in terms of the volumes and spatial control over the injectate that is ultimately delivered to the LV wall.

Perspective

Important milestones have been reached for intramyocardial biomaterial injection therapy during the first decade since the introduction of this concept. Particularly in the past five years, forms of this type of therapy have proven compelling enough to justify the initiation of clinical trials. For this type of therapy to become a routine option for MI patients, like coronary artery bypass grafting or stenting, there will, of course, need to be compelling data from future clinical trials. Furthermore, for clinical success and widespread adoption, it appears that further progress will need to occur in understanding the mechanisms by which injection therapy may benefit and preserve cardiac function, and how to improve material design to leverage this knowledge. From a practical application perspective, improvements in material properties, injection strategies, imaging, and modeling all can help to improve the efficacy of the therapy to a point where its clinical potential might be realized.

More readily available, information-rich cardiac imaging strategies should complement the development of biomaterial injection therapy. Such advancements would provide better information to correlate the topography of injectate delivery with the local state of the cardiac tissue, allowing the development of algorithms that optimize injection maps for improved, patient-specific functional outcomes. To realize the potential offered by imaging advancements, better delivery methods that can effectively deliver precise injectate patterns within targeted tissue regions will be essential. As noted in this review, significant progress is being made in this area, but much room remains for innovation. In terms of the nature of the injectate, the field continues to offer biomaterials scientists and engineers an intriguing design landscape. The classic trade-offs between bioactive natural materials and highly controllable synthetic materials characterize much of the literature to date. As with many other biomaterial applications, designs that can capture the strengths of each material approach would be desirable. The specific design criteria will remain in flux as mechanistic questions and delivery strategies are explored.

Often underestimated in its importance for the adoption of such new interventional approaches is the design of the early clinical trials. This is apparent in the few approaches that have progressed to this stage for biomaterial injection therapy, as investigators and regulators seek to design trials that will provide an appropriate risk/benefit profile, but still apply the therapy in a setting where the benefit is pronounced and readily demonstrated. Often this means application in patients with poorer prognoses, (who may be receiving concurrent gold-standard therapy) and the application of the new therapy in a less aggressive fashion. The clinical trials to date suggest that study design may have failed to provide a scenario that allowed the benefit of biomaterial injection therapy to be clearly demonstrated. This is clearly a statement made from the perspective that biomaterial injection therapy holds promise, but is based on observations that many of the parameters employed to date in the clinic may have been suboptimal. For instance, the injectate volume, achieved injectate pattern, patient selection criteria, and time of intervention all are subject to criticism based on pre-clinical studies and modeling results. Further, clinical trials reported to date have used the relatively bland material, alginate. While attractive from a regulatory perspective, this review has discussed the broad array of alternative natural and synthetic materials that would be more attractive from a variety of perspectives. In spite of the early clinical failures in terms of their primary endpoints, it is worth recalling that the AUGMENT-HF trial did demonstrate benefit in secondary endpoints (mean peak VO_2 and mean 6 min walk distance), providing encouragement that the early results will serve as a baseline for future advancement.

In considering the future, this review carried a bias in that it focused exclusively on acellular biomaterial injection strategies, whose main function is to provide mechanical support to the LV wall. This class of materials included functional biomaterials whose bioactive components are innate or are covalently attached to the principal material. Not considered were injectable biomaterials that serve principally as vehicles for the delivery of bioactive factors including pharmaceuticals, growth factors or cells. Interested readers may refer to recent reviews that provide good coverage of biomaterials designed for controlled release and delivery in the heart [12, 123, 124]. Although biomaterial injection therapy has repeatedly demonstrated efficacy in animal models, the primary effect and endpoint across

the many studies is the preservation of cardiac function. However, the ultimate goal for MI treatment is to regenerate myocardial tissue and restore the cardiac function to pre-infarct levels. Recent advances in cell-based cardiac therapy have demonstrated some promise that cardiomyocyte populations may be restored in the infarcted LV [125–127]. There is potential to combine the mechanical features inherent in the materials of this review with the pharmaceutical and biological features developing rapidly as well to create injection strategies capable of additional efficacy, albeit with potential added regulatory burden.

The application of biomaterial injection therapy to patients other than those with ischemic cardiomyopathy was also not addressed. There may be value in using this general strategy in patients with cardiac diseases characterized by mechanically weaker ventricular walls where the mechanical or added biological effects discussed above might preserve remaining cardiac function and maintain a better overall condition while awaiting cardiac transplantation.

Conclusion

Recent progress in the field of intramyocardial biomaterial injection therapy continues to entice the broader biomedical community that this relatively straightforward strategy offers the potential to mitigate post-MI LV remodeling and might supplement revascularization therapy to reduce the number of patients progressing to end-stage ischemic cardiomyopathy. Future developments will likely focus on gaining a deeper and more comprehensive understanding of the underlying mechanisms through which this intervention alters pathologic ventricular remodeling. Further exploration of delivery methods coupled with imaging strategies should help maximize functional benefits. Finally, for biomaterials scientists, the field offers numerous challenges to design injectable materials that meet an intriguing array of design constraints dictated by both delivery strategy and understanding of the underlying physiological processes.

Supplementary Material

Refer to Web version on PubMed Central for supplementary material.

Acknowledgments

This work was financially supported by the US National Institutes of Health (grant R01 HL105911) and the McGowan Institute for Regenerative Medicine. The authors would like to thank Dr. Tanchen Ren for assistance in preparing illustrations.

References

1. WHO, Global status report on noncommunicable diseases 2014. World Health Organization; Geneva: 2014.
2. Xu J, Murphy SL, Kochanek KD, Bastian BA. Deaths: Final Data for 2013. Natl Vital Stat Rep. 2016:1–119.
3. Christman KL, Fok HH, Sievers RE, Fang Q, Lee RJ. Fibrin glue alone and skeletal myoblasts in a fibrin scaffold preserve cardiac function after myocardial infarction. Tissue Eng. 2004:403–409. [PubMed: 15165457]

4. Christman KL, Vardanian AJ, Fang Q, Sievers RE, Fok HH, Lee RJ. Injectable fibrin scaffold improves cell transplant survival, reduces infarct expansion, and induces neovasculature formation in ischemic myocardium. J Am Coll Cardiol. 2004:654–660. [PubMed: 15358036]
5. Wall ST, Walker JC, Healy KE, Ratcliffe MB, Guccione JM. Theoretical impact of the injection of material into the myocardium: a finite element model simulation. Circulation. 2006:2627–2635. [PubMed: 17130342]
6. Tous E, Purcell B, Ifkovits J, Burdick J. Injectable Acellular Hydrogels for Cardiac Repair. J Cardiovasc Transl Res. 2011:528–542. [PubMed: 21710332]
7. Rane AA, Christman KL. Biomaterials for the treatment of myocardial infarction: a 5-year update. J Am Coll Cardiol. 2011:2615–2629. [PubMed: 22152947]
8. Nelson DM, Ma Z, Fujimoto KL, Hashizume R, Wagner WR. Intra-myocardial biomaterial injection therapy in the treatment of heart failure: Materials, outcomes and challenges. Acta Biomater. 2011:1–15. [PubMed: 20619368]
9. BioLineRx, L. Safety and Feasibility of the Injectable BL-1040 Implant. https://clinicaltrials.gov/ct2/show/NCT00557531 2009(accessed 2016.11.15)
10. Leor J, Tuvia S, Guetta V, Manczur F, Castel D, Willenz U, Petnehazy O, Landa N, Feinberg MS, Konen E, Goitein O, Tsur-Gang O, Shaul M, Klapper L, Cohen S. Intracoronary injection of in situ forming alginate hydrogel reverses left ventricular remodeling after myocardial infarction in Swine. J Am Coll Cardiol. 2009:1014–1023. [PubMed: 19729119]
11. Frey N, Linke A, Suselbeck T, Muller-Ehmsen J, Vermeersch P, Schoors D, Rosenberg M, Bea F, Tuvia S, Leor J. Intracoronary delivery of injectable bioabsorbable scaffold (IK-5001) to treat left ventricular remodeling after ST-elevation myocardial infarction: a first-in-man study. Circ Cardiovasc Interv. 2014:806–812. [PubMed: 25351198]
12. O'Neill HS, Gallagher LB, O'Sullivan J, Whyte W, Curley C, Dolan E, Hameed A, O'Dwyer J, Payne C, O'Reilly D, Ruiz-Hernandez E, Roche ET, O'Brien FJ, Cryan SA, Kelly H, Murphy B, Duffy GP. Biomaterial-Enhanced Cell and Drug Delivery: Lessons Learned in the Cardiac Field and Future Perspectives. Adv Mater. 2016:5648–5661. [PubMed: 26840955]
13. B.B. LLC. IK-5001 for the Prevention of Remodeling of the Ventricle and Congestive Heart Failure After Acute Myocardial Infarction (PRESERVATION 1). 2010. https://clinicaltrials.gov/ct2/show/NCT01226563(accessed 2016.11.30)
14. Rao SV, Zeymer U, Douglas PS, Al-Khalidi H, Liu J, Gibson CM, Harrison RW, Joseph DS, Heyrman R, Krucoff MW. A randomized, double-blind, placebo-controlled trial to evaluate the safety and effectiveness of intracoronary application of a novel bioabsorbable cardiac matrix for the prevention of ventricular remodeling after large ST-segment elevation myocardial infarction: Rationale and design of the PRESERVATION I trial. Am Heart J. 2015:929–937. [PubMed: 26542501]
15. Zeymer, U., Rao, SV., Krucoff, MW. A placebo-controlled, multicenter, randomized, doubleblind trial to evaluate the safety and effectiveness of IK-5001 (Bioabsorbable Cardiac Matrix [BCM] for the prevention of remodeling of the ventricle and congestive heart failure after acute myocardial infarction. 2015. https://www.escardio.org/static_file/Escardio/Press-media/Press%20releases/2015/Congress/PRESERVATION_Zeymer.pdf(accessed 2016.10.30)
16. Sabbah HN, Wang M, Jiang A, Ilsar I, Sabbah MS, Helgerson S, Peterson R, Tarazona N, Lee R. Abstract 4050: Circumferential Mid-Ventricular Intramyocardial Injections of Alginate Hydrogel Improve Left Ventricular Function and Prevent Progressive Remodeling in Dogs With Chronic Heart Failure. Circulation. 2016:S912–S912.
17. Sabbah HN, Wang M, Gupta RC, Rastogi S, Ilsar I, Sabbah MS, Kohli S, Helgerson S, Lee RJ. Augmentation of Left Ventricular Wall Thickness With Alginate Hydrogel Implants Improves Left Ventricular Function and Prevents Progressive Remodeling in Dogs With Chronic Heart Failure. JACC Heart Fail. 2013:252–258. [PubMed: 23998003]
18. Lee RJ, Hinson A, Helgerson S, Bauernschmitt R, Sabbah HN. Polymer-based restoration of left ventricular mechanics. Cell Transplant. 2013:529–533. [PubMed: 22469060]
19. L.H. Inc. A Randomized, Controlled Study to Evaluate Algisyl-LVR™ as a Method of Left Ventricular Augmentation for Heart Failure (AUGMENT-HF). 2009. https://clinicaltrials.gov/ct2/show/NCT00847964(accessed 2016.12.05)

20. Lee LC, Zhihong Z, Hinson A, Guccione JM. Reduction in left ventricular wall stress and improvement in function in failing hearts using Algisyl-LVR. J Vis Exp. 2013
21. Lee LC, Wall ST, Klepach D, Ge L, Zhang Z, Lee RJ, Hinson A, Gorman JH 3rd, Gorman RC, Guccione JM. Algisyl-LVR with coronary artery bypass grafting reduces left ventricular wall stress and improves function in the failing human heart. Int J Cardiol. 2013:2022–2028. [PubMed: 23394895]
22. Mann DL, Lee RJ, Coats AJ, Neagoe G, Dragomir D, Pusineri E, Piredda M, Bettari L, Kirwan BA, Dowling R, Volterrani M, Solomon SD, Sabbah HN, Hinson A, Anker SD. One-year follow-up results from AUGMENT-HF: a multicentre randomized controlled clinical trial of the efficacy of left ventricular augmentation with Algisyl in the treatment of heart failure. Eur J Heart Fail. 2016:314–325.
23. Singelyn JM, DeQuach JA, Seif-Naraghi SB, Littlefield RB, Schup-Magoffin PJ, Christman KL. Naturally derived myocardial matrix as an injectable scaffold for cardiac tissue engineering. Biomaterials. 2009:5409–5416. [PubMed: 19608268]
24. Ventrix, I. A Study of VentriGel in Early and Late Post-myocardial Infarction Patients. 2014. https://clinicaltrials.gov/ct2/show/NCT02305602(accessed 2016.11.08)
25. Seif-Naraghi SB, Salvatore MA, Schup-Magoffin PJ, Hu DP, Christman KL. Design and characterization of an injectable pericardial matrix gel: a potentially autologous scaffold for cardiac tissue engineering. Tissue Eng Part A. 2010:2017–2027. [PubMed: 20100033]
26. Badylak SF, Freytes DO, Gilbert TW. Extracellular matrix as a biological scaffold material: Structure and function. Acta Biomater. 2009:1–13. [PubMed: 18938117]
27. Badylak SF, Freytes DO, Gilbert TW. Reprint of: Extracellular matrix as a biological scaffold material: Structure and function. Acta Biomater. 2015:S17–26. [PubMed: 26235342]
28. Meng FW, Slivka PF, Dearth CL, Badylak SF. Solubilized extracellular matrix from brain and urinary bladder elicits distinct functional and phenotypic responses in macrophages. Biomaterials. 2015:131–140.
29. Singelyn JM, Sundaramurthy P, Johnson TD, Schup-Magoffin PJ, Hu DP, Faulk DM, Wang J, Mayle KM, Bartels K, Salvatore M, Kinsey AM, DeMaria AN, Dib N, Christman KL. Catheter-Deliverable Hydrogel Derived From Decellularized Ventricular Extracellular Matrix Increases Endogenous Cardiomyocytes and Preserves Cardiac Function Post-Myocardial Infarction. J Am Coll Cardiol. 2012:751–763. [PubMed: 22340268]
30. Seif-Naraghi SB, Singelyn JM, Salvatore MA, Osborn KG, Wang JJ, Sampat U, Kwan OL, Strachan GM, Wong J, Schup-Magoffin PJ, Braden RL, Bartels K, DeQuach JA, Preul M, Kinsey AM, DeMaria AN, Dib N, Christman KL. Safety and efficacy of an injectable extracellular matrix hydrogel for treating myocardial infarction. Sci Transl Med. 2013:173ra125.
31. Vu TD, Pal SN, Ti LK, Martinez EC, Rufaihah AJ, Ling LH, Lee CN, Richards AM, Kofidis T. An autologous platelet-rich plasma hydrogel compound restores left ventricular structure, function and ameliorates adverse remodeling in a minimally invasive large animal myocardial restoration model: a translational approach: Vu and Pal “Myocardial Repair: PRP, Hydrogel and Supplements”. Biomaterials. 2015:27–35.
32. Eckhouse SR, Purcell BP, McGarvey JR, Lobb D, Logdon CB, Doviak H, O’Neill JW, Shuman JA, Novack CP, Zellars KN, Pettaway S, Black RA, Khakoo A, Lee T, Mukherjee R, Gorman JH, Gorman RC, Burdick JA, Spinale FG. Local hydrogel release of recombinant TIMP-3 attenuates adverse left ventricular remodeling after experimental myocardial infarction. Sci Transl Med. 2014:223ra221.
33. Dorsey SM, McGarvey JR, Wang H, Nikou A, Arama L, Koomalsingh KJ, Kondo N, Gorman JH 3rd, Pilla JJ, Gorman RC, Wenk JF, Burdick JA. MRI evaluation of injectable hyaluronic acid-based hydrogel therapy to limit ventricular remodeling after myocardial infarction. Biomaterials. 2015:65–75.
34. Tous E, Ifkovits JL, Koomalsingh KJ, Shuto T, Soeda T, Kondo N, Gorman JH 3rd, Gorman RC, Burdick JA. Influence of injectable hyaluronic acid hydrogel degradation behavior on infarction-induced ventricular remodeling. Biomacromolecules. 2011:4127–4135. [PubMed: 21967486]
35. Rodell CB, Lee ME, Wang H, Takebayashi S, Takayama T, Kawamura T, Arkles JS, Dusaj NN, Dorsey SM, Witschey WR, Pilla JJ, Gorman JH 3rd, Wenk JF, Burdick JA, Gorman RC. Injectable

Shear-Thinning Hydrogels for Minimally Invasive Delivery to Infarcted Myocardium to Limit Left Ventricular Remodeling. Circ Cardiovasc Interv. 2016:1268–1276.

36. Morita M, Eckert CE, Matsuzaki K, Noma M, Ryan LP, Burdick JA, Jackson BM, Gorman JH 3rd, Sacks MS, Gorman RC. Modification of infarct material properties limits adverse ventricular remodeling. Ann Thorac Surg. 2011:617–624. [PubMed: 21801916]
37. McGarvey JR, Kondo N, Witschey WR, Takebe M, Aoki C, Burdick JA, Spinale FG, Gorman JH 3rd, Pilla JJ, Gorman RC. Injectable microsphere gel progressively improves global ventricular function, regional contractile strain, and mitral regurgitation after myocardial infarction. Ann Thorac Surg. 2015:597–603. [PubMed: 25524397]
38. McGarvey JR, Pettaway S, Shuman JA, Novack CP, Zellars KN, Freels PD, Echols RL Jr, Burdick JA, Gorman JH 3rd, Gorman RC, Spinale FG. Targeted injection of a biocomposite material alters macrophage and fibroblast phenotype and function following myocardial infarction: relation to left ventricular remodeling. J Pharmacol Exp Ther. 2014:701–709. [PubMed: 25022514]
39. Dixon JA, Gorman RC, Stroud RE, Mukherjee R, Meyer EC, Baker NL, Morita M, Hamamoto H, Ryan LP, Gorman JH 3rd, Spinale FG. Targeted regional injection of biocomposite microspheres alters post-myocardial infarction remodeling and matrix proteolytic pathways. Circulation. 2011:S35–45. [PubMed: 21911817]
40. Bastings MM, Koudstaal S, Kieltyka RE, Nakano Y, Pape AC, Feyen DA, van Slochteren FJ, Doevendans PA, Sluijter JP, Meijer EW, Chamuleau SA, Dankers PY. A fast pH-switchable and self-healing supramolecular hydrogel carrier for guided, local catheter injection in the infarcted myocardium. Adv Healthc Mater. 2014:70–78. [PubMed: 23788397]
41. Lin YD, Chang MY, Cheng B, Liu YW, Lin LC, Chen JH, Hsieh PC. Injection of Peptide nanogels preserves postinfarct diastolic function and prolongs efficacy of cell therapy in pigs. Tissue Eng Part A. 2015:1662–1671. [PubMed: 25686878]
42. Soucy KG, Smith EF, Monreal G, Rokosh G, Keller BB, Yuan F, Matheny RG, Fallon AM, Lewis BC, Sherwood LC, Sobieski MA, Giridharan GA, Koenig SC, Slaughter MS. Feasibility study of particulate extracellular matrix (P-ECM) and left ventricular assist device (HVAD) therapy in chronic ischemic heart failure bovine model. ASAIO J. 2015:161–169. [PubMed: 25423120]
43. Swindle MM, Makin A, Herron AJ, Clubb FJ Jr, Frazier KS. Swine as models in biomedical research and toxicology testing. Vet Pathol. 2012:344–356. [PubMed: 21441112]
44. Kassab GS, Fung YC. Topology and dimensions of pig coronary capillary network. American Journal of Physiology - Heart and Circulatory Physiology. 1994:H319–H325.
45. Bainey KR, Armstrong PW. Ameliorating reperfusion injury in STEMI: dead or alive? Eur Heart J. 2014:2504–2506. [PubMed: 24875796]
46. Kapur NK, Paruchuri V, Urbano-Morales JA, Mackey EE, Daly GH, Qiao X, Pandian N, Perides G, Karas RH. Mechanically unloading the left ventricle before coronary reperfusion reduces left ventricular wall stress and myocardial infarct size. Circulation. 2013:328–336. [PubMed: 23766351]
47. Fordyce CB, Gersh BJ, Stone GW, Granger CB. Novel therapeutics in myocardial infarction: targeting microvascular dysfunction and reperfusion injury. Trends Pharmacol Sci. 2015:605–616. [PubMed: 26148636]
48. Sack KL, Davies NH, Guccione JM, Franz T. Personalised computational cardiology: Patient-specific modelling in cardiac mechanics and biomaterial injection therapies for myocardial infarction. Heart Fail Rev. 2016
49. Kichula ET, Wang H, Dorsey SM, Szczesny SE, Elliott DM, Burdick JA, Wenk JF. Experimental and computational investigation of altered mechanical properties in myocardium after hydrogel injection. Ann Biomed Eng. 2014:1546–1556. [PubMed: 24271262]
50. Wenk JF, Eslami P, Zhang Z, Xu C, Kuhl E, Gorman JH Iii, Robb JD, Ratcliffe MB, Gorman RC, Guccione JM. A Novel Method for Quantifying the In-Vivo Mechanical Effect of Material Injected Into a Myocardial Infarction. Ann Thorac Surg. 2011:935–941.
51. Toussaint N, Stoeck CT, Schaeffter T, Kozerke S, Sermesant M, Batchelor PG. In vivo human cardiac fibre architecture estimation using shape-based diffusion tensor processing. Med Image Anal. 2013:1243–1255. [PubMed: 23523287]

52. Lee LC, Wall ST, Genet M, Hinson A, Guccione JM. Bioinjection treatment: effects of post-injection residual stress on left ventricular wall stress. J Biomech. 2014:3115–3119. [PubMed: 25065728]
53. Kortsmit J, Davies NH, Miller R, Zilla P, Franz T. Computational predictions of improved of wall mechanics and function of the infarcted left ventricle at early and late remodelling stages. Adv Biomech Appl. 2013:41–55.
54. Miller R, Davies NH, Kortsmit J, Zilla P, Franz T. Outcomes of myocardial infarction hydrogel injection therapy in the human left ventricle dependent on injectate distribution. Int J Numer Method Biomed Eng. 2013:870–884. [PubMed: 23640777]
55. Kadner K, Dobner S, Franz T, Bezuidenhout D, Sirry MS, Zilla P, Davies NH. The beneficial effects of deferred delivery on the efficiency of hydrogel therapy post myocardial infarction. Biomaterials. 2012:2060–2066. [PubMed: 22153866]
56. Cain PA, Ahl R, Hedstrom E, Ugander M, Allansdotter-Johnsson A, Friberg P, Arheden H. Age and gender specific normal values of left ventricular mass, volume and function for gradient echo magnetic resonance imaging: a cross sectional study. BMC Med Imaging. 2009:2. [PubMed: 19159437]
57. Foppa M, Duncan BB, Rohde LE. Echocardiography-based left ventricular mass estimation. How should we define hypertrophy? Cardiovasc Ultrasound. 2005:17. [PubMed: 15963236]
58. Wise P, Davies NH, Sirry MS, Kortsmit J, Dubuis L, Chai CK, Baaijens FP, Franz T. Excessive volume of hydrogel injectates may compromise the efficacy for the treatment of acute myocardial infarction. Int J Numer Method Biomed Eng. 2016
59. Jugdutt, BI., Dhalla, NS. Cardiac Remodeling: Molecular Mechanisms. Springer; New York: 2013.
60. Landa N, Miller L, Feinberg MS, Holbova R, Shachar M, Freeman I, Cohen S, Leor J. Effect of injectable alginate implant on cardiac remodeling and function after recent and old infarcts in rat. Circulation. 2008:1388–1396. [PubMed: 18316487]
61. Yoshizumi T, Zhu Y, Jiang H, D'Amore A, Sakaguchi H, Tchao J, Tobita K, Wagner WR. Timing effect of intramyocardial hydrogel injection for positively impacting left ventricular remodeling after myocardial infarction. Biomaterials. 2016:182–193.
62. Fujimoto KL, Ma Z, Nelson DM, Hashizume R, Guan J, Tobita K, Wagner WR. Synthesis, characterization and therapeutic efficacy of a biodegradable, thermoresponsive hydrogel designed for application in chronic infarcted myocardium. Biomaterials. 2009:4357–4368. [PubMed: 19487021]
63. Yoon SJ, Fang YH, Lim CH, Kim BS, Son HS, Park Y, Sun K. Regeneration of ischemic heart using hyaluronic acid-based injectable hydrogel. J Biomed Mater Res B Appl Biomater. 2009:163–171. [PubMed: 19399850]
64. Mukherjee R, Zavadzkas JA, Saunders SM, McLean JE, Jeffords LB, Beck C, Stroud RE, Leone AM, Koval CN, Rivers WT, Basu S, Sheehy A, Michal G, Spinale FG. Targeted myocardial microinjections of a biocomposite material reduces infarct expansion in pigs. Ann Thorac Surg. 2008:1268–1276. [PubMed: 18805174]
65. Wang H, Zhang X, Li Y, Ma Y, Zhang Y, Liu Z, Zhou J, Lin Q, Wang Y, Duan C, Wang C. Improved myocardial performance in infarcted rat heart by co-injection of basic fibroblast growth factor with temperature-responsive Chitosan hydrogel. J Heart Lung Transplant. 2010:881–887. [PubMed: 20466563]
66. Zhao ZQ, Puskas JD, Xu D, Wang NP, Mosunjac M, Guyton RA, Vinten-Johansen J, Matheny R. Improvement in cardiac function with small intestine extracellular matrix is associated with recruitment of C-kit cells, myofibroblasts, and macrophages after myocardial infarction. J Am Coll Cardiol. 2010:1250–1261. [PubMed: 20298933]
67. Chen WCW, Wang Z, Missinato MA, Park DW, Long DW, Liu HJ, Zeng X, Yates NA, Kim K, Wang Y. Decellularized zebrafish cardiac extracellular matrix induces mammalian heart regeneration. Science Advances. 2016
68. Wassenaar JW, Gaetani R, Garcia JJ, Braden RL, Luo CG, Huang D, DeMaria AN, Omens JH, Christman KL. Evidence for Mechanisms Underlying the Functional Benefits of a Myocardial Matrix Hydrogel for Post-MI Treatment. J Am Coll Cardiol. 2016:1074–1086. [PubMed: 26940929]

69. Suarez SL, Rane AA, Munoz A, Wright AT, Zhang SX, Braden RL, Almutairi A, McCulloch AD, Christman KL. Intramyocardial injection of hydrogel with high interstitial spread does not impact action potential propagation. Acta Biomater. 2015:13–22.
70. Sun Y. Myocardial repair/remodelling following infarction: roles of local factors. Cardiovasc Res. 2009:482–490. [PubMed: 19050008]
71. Delcayre C, Silvestre JS, Garnier A, Oubenaissa A, Cailmail S, Tatara E, Swynghedauw B, Robert V. Cardiac aldosterone production and ventricular remodeling. Kidney Int. 2000:1346–1351.
72. Dostal DE, Baker KM. The cardiac renin-angiotensin system: conceptual, or a regulator of cardiac function? Circ Res. 1999:643–650. [PubMed: 10506489]
73. Tinkel J, Hassanain H, Khouri SJ. Cardiovascular antioxidant therapy: a review of supplements, pharmacotherapies, and mechanisms. Cardiol Rev. 2012:77–83. [PubMed: 22293859]
74. Pfeffer MA, Braunwald E. Ventricular remodeling after myocardial infarction. Experimental observations and clinical implications. Circulation. 1990:1161–1172. [PubMed: 2138525]
75. Okada M, Payne TR, Oshima H, Momoi N, Tobita K, Huard J. Differential efficacy of gels derived from small intestinal submucosa as an injectable biomaterial for myocardial infarct repair. Biomaterials. 2010:7678–7683. [PubMed: 20674011]
76. Sirry MS, Davies NH, Kadner K, Dubuis L, Saleh MG, Meintjes EM, Spottiswoode BS, Zilla P, Franz T. Micro-structurally detailed model of a therapeutic hydrogel injectate in a rat biventricular cardiac geometry for computational simulations. Comput Methods Biomech Biomed Eng. 2015:325–331.
77. Rouillard AD, Holmes JW. Coupled agent-based and finite-element models for predicting scar structure following myocardial infarction. Prog Biophys Mol Biol. 2014:235–243. [PubMed: 25009995]
78. Rane AA, Chuang JS, Shah A, Hu DP, Dalton ND, Gu Y, Peterson KL, Omens JH, Christman KL. Increased infarct wall thickness by a bio-inert material is insufficient to prevent negative left ventricular remodeling after myocardial infarction. PLoS One. 2011:e21571. [PubMed: 21731777]
79. Dobner S, Bezuidenhout D, Govender P, Zilla P, Davies N. A synthetic non-degradable polyethylene glycol hydrogel retards adverse post-infarct left ventricular remodeling. J Card Fail. 2009:629–636. [PubMed: 19700140]
80. Mihic A, Cui Z, Wu J, Vlacic G, Miyagi Y, Li SH, Lu S, Sung HW, Weisel RD, Li RK. A Conductive Polymer Hydrogel Supports Cell Electrical Signaling and Improves Cardiac Function After Implantation into Myocardial Infarct. Circulation. 2015:772–784.
81. Cui H, Liu Y, Cheng Y, Zhang Z, Zhang P, Chen X, Wei Y. In Vitro Study of Electroactive Tetraaniline-Containing Thermosensitive Hydrogels for Cardiac Tissue Engineering. Biomacromolecules. 2014
82. Baei P, Jalili-Firoozinezhad S, Rajabi-Zeleti S, Tafazzoli-Shadpour M, Baharvand H, Aghdami N. Electrically conductive gold nanoparticle-chitosan thermosensitive hydrogels for cardiac tissue engineering. Mater Sci Eng C Mater Biol Appl. 2016:131–141. [PubMed: 27040204]
83. Annabi N, Shin SR, Tamayol A, Miscuglio M, Bakooshli MA, Assmann A, Mostafalu P, Sun JY, Mithieux S, Cheung L, Tang XS, Weiss AS, Khademhosseini A. Highly Elastic and Conductive Human-Based Protein Hybrid Hydrogels. Adv Mater. 2016:40–49. [PubMed: 26551969]
84. Reis LA, Chiu LL, Wu J, Feric N, Laschinger C, Momen A, Li RK, Radisic M. Hydrogels with integrin-binding angiopoietin-1-derived peptide, QHREDGS, for treatment of acute myocardial infarction. Circ Heart Fail. 2015:333–341. [PubMed: 25632037]
85. Li J, Shu Y, Hao T, Wang Y, Qian Y, Duan C, Sun H, Lin Q, Wang C. A chitosan-glutathione based injectable hydrogel for suppression of oxidative stress damage in cardiomyocytes. Biomaterials. 2013:9071–9081. [PubMed: 24001992]
86. Rocca DG, Willenberg BJ, Qi Y, Simmons CS, Rubiano A, Ferreira LF, Huo T, Petersen JW, Ruchaya PJ, Wate PS, Wise EA, Handberg EM, Cogle CR, Batich CD, Byrne BJ, Pepine CJ. An injectable capillary-like microstructured alginate hydrogel improves left ventricular function after myocardial infarction in rats. Int J Cardiol. 2016:149–154.
87. Brown BN, Valentin JE, Stewart-Akers AM, McCabe GP, Badylak SF. Macrophage phenotype and remodeling outcomes in response to biologic scaffolds with and without a cellular component. Biomaterials. 2009:1482–1491. [PubMed: 19121538]

88. Johnson TD, Dequach JA, Gaetani R, Ungerleider J, Elhag D, Nigam V, Behfar A, Christman KL. Human versus porcine tissue sourcing for an injectable myocardial matrix hydrogel. Biomater Sci. 2014:735–744.

89. Paulis LE, Geelen T, Kuhlmann MT, Coolen BF, Schafers M, Nicolay K, Strijkers GJ. Distribution of lipid-based nanoparticles to infarcted myocardium with potential application for MRI-monitored drug delivery. J Control Release. 2012:276–285.

90. Lundy DJ, Chen KH, Toh EK, Hsieh PC. Distribution of Systemically Administered Nanoparticles Reveals a Size-Dependent Effect Immediately following Cardiac Ischaemia-Reperfusion Injury. Sci Rep. 2016:25613. [PubMed: 27161857]

91. Yao C, Shi X, Lin X, Shen L, Xu D, Feng Y. Increased cardiac distribution of mono-PEGylated Radix Ophiopogonis polysaccharide in both myocardial infarction and ischemia/reperfusion rats, Int. J Nanomedicine. 2015:409–418.

92. Dvir T, Bauer M, Schroeder A, Tsui JH, Anderson DG, Langer R, Liao R, Kohane DS. Nanoparticles targeting the infarcted heart. Nano Lett. 2011:4411–4414. [PubMed: 21899318]

93. Nguyen MM, Carlini AS, Chien MP, Sonnenberg S, Luo C, Braden RL, Osborn KG, Li Y, Gianneschi NC, Christman KL. Enzyme-Responsive Nanoparticles for Targeted Accumulation and Prolonged Retention in Heart Tissue after Myocardial Infarction. Adv Mater. 2015:5547–5552. [PubMed: 26305446]

94. Xu G, Wang X, Deng C, Teng X, Suuronen EJ, Shen Z, Zhong Z. Injectable biodegradable hybrid hydrogels based on thiolated collagen and oligo(acryloyl carbonate)-poly(ethylene glycol)-oligo(acryloyl carbonate) copolymer for functional cardiac regeneration. Acta Biomater. 2015:55–64.

95. Bai X, Fang R, Zhang S, Shi X, Wang Z, Chen X, Yang J, Hou X, Nie Y, Li Y, Tian W. Self-cross-linkable hydrogels composed of partially oxidized alginate and gelatin for myocardial infarction repair. J Bioact Compatible Polym. 2013:126–140.

96. Rodell CB, Kaminski AL, Burdick JA. Rational design of network properties in guest-host assembled and shear-thinning hyaluronic acid hydrogels. Biomacromolecules. 2013:4125–4134. [PubMed: 24070551]

97. Gaffey AC, Chen MH, Venkataraman CM, Trubelja A, Rodell CB, Dinh PV, Hung G, MacArthur JW, Soopan RV, Burdick JA, Atluri P. Injectable shear-thinning hydrogels used to deliver endothelial progenitor cells, enhance cell engraftment, and improve ischemic myocardium. J Thorac Cardiovasc Surg. 2015:1268–1276. [PubMed: 26293548]

98. Rodell CB, MacArthur JW, Dorsey SM, Wade RJ, Wang LL, Woo YJ, Burdick JA. Shear-Thinning Supramolecular Hydrogels with Secondary Autonomous Covalent Crosslinking to Modulate Viscoelastic Properties In Vivo. Adv Funct Mater. 2015:636–644. [PubMed: 26526097]

99. Ren S, Jiang X, Li Z, Wen Y, Chen D, Li X, Zhang X, Zhuo R, Chu H. Physical Properties of Poly(N-isopropylacrylamide) Hydrog el Promote its Effects on Cardiac Protection after Myocardial Infarction. J Int Med Res. 2012:2167–2182. [PubMed: 23321174]

100. Zhu Y, Jiang H, Ye SH, Yoshizumi T, Wagner WR. Tailoring the degradation rates of thermally responsive hydrogels designed for soft tissue injection by varying the autocatalytic potential. Biomaterials. 2015:484–493.

101. Nelson DM, Hashizume R, Yoshizumi T, Blakney AK, Ma Z, Wagner WR. Intramyocardial injection of a synthetic hydrogel with delivery of bFGF and IGF1 in a rat model of ischemic cardiomyopathy. Biomacromolecules. 2014:1–11.

102. Ifkovits JL, Tous E, Minakawa M, Morita M, Robb JD, Koomalsingh KJ, Gorman JH 3rd, Gorman RC, Burdick JA. Injectable hydrogel properties influence infarct expansion and extent of postinfarction left ventricular remodeling in an ovine model. Proc Natl Acad Sci U S A. 2010:11507–11512. [PubMed: 20534527]

103. Williams C, Budina E, Stoppel WL, Sullivan KE, Emani S, Emani SM, Black LD 3rd. Cardiac extracellular matrix-fibrin hybrid scaffolds with tunable properties for cardiovascular tissue engineering. Acta Biomater. 2015:84–95.

104. Singelyn JM, Christman KL. Modulation of Material Properties of a Decellularized Myocardial Matrix Scaffold. Macromol Biosci. 2011:731–738. [PubMed: 21322109]

105. Pinney JR, Du KT, Ayala P, Fang Q, Sievers RE, Chew P, Delrosario L, Lee RJ, Desai TA. Discrete microstructural cues for the attenuation of fibrosis following myocardial infarction. Biomaterials. 2014:8820–8828. [PubMed: 25047625]
106. Chang MY, Yang YJ, Chang CH, Tang AC, Liao WY, Cheng FY, Yeh CS, Lai JJ, Stayton PS, Hsieh PC. Functionalized nanoparticles provide early cardioprotection after acute myocardial infarction. J Control Release. 2013:287–294. [PubMed: 23665256]
107. Zhu Y, Wood NA, Fok K, Yoshizumi T, Park DW, Jiang H, Schwartzman DS, Zenati MA, Uchibori T, Wagner WR, Riviere CN. Design of a Coupled Thermoresponsive Hydrogel and Robotic System for Postinfarct Biomaterial Injection Therapy. Ann Thorac Surg. 2016:780–786.
108. Griffin DR, Weaver WM, Scumpia PO, Di Carlo D, Segura T. Accelerated wound healing by injectable microporous gel scaffolds assembled from annealed building blocks. Nat Mater. 2015:737–744. [PubMed: 26030305]
109. Bencherif SA, Sands RW, Bhatta D, Arany P, Verbeke CS, Edwards DA, Mooney DJ. Injectable preformed scaffolds with shape-memory properties. Proc Natl Acad Sci U S A. 2012:19590–19595. [PubMed: 23150549]
110. Krebs MD, Sutter KA, Lin AS, Guldberg RE, Alsberg E. Injectable poly(lactic-co-glycolic) acid scaffolds with in situ pore formation for tissue engineering. Acta Biomater. 2009:2847–2859. [PubMed: 19446056]
111. Sussman EM, Halpin MC, Muster J, Moon RT, Ratner BD. Porous implants modulate healing and induce shifts in local macrophage polarization in the foreign body reaction. Ann Biomed Eng. 2014:1508–1516. [PubMed: 24248559]
112. Hwang H, Kwon J, Oh PS, Lee TK, Na KS, Lee CM, Jeong HS, Lim ST, Sohn MH, Jeong HJ. Peptide-loaded nanoparticles and radionuclide imaging for individualized treatment of myocardial ischemia. Radiology. 2014:160–167. [PubMed: 24927328]
113. Danila D, Johnson E, Kee P. CT imaging of myocardial scars with collagen-targeting gold nanoparticles. Nanomed Nanotechnol Biol Med 1067–1076.
114. Taruttis A, Ntziachristos V. Advances in real-time multispectral optoacoustic imaging and its applications. Nature Photonics. 2015:219–227.
115. Park DW, Ye SH, Jiang HB, Dutta D, Nonaka K, Wagner WR, Kim K. In vivo monitoring of structural and mechanical changes of tissue scaffolds by multi-modality imaging. Biomaterials. 2014:7851–7859. [PubMed: 24951048]
116. Appel AA, Anastasio MA, Larson JC, Brey EM. Imaging challenges in biomaterials and tissue engineering. Biomaterials. 2013:6615–6630. [PubMed: 23768903]
117. Dorsey SM, Haris M, Singh A, Witschey WRT, Rodell CB, Kogan F, Reddy R, Burdick JA. Visualization of Injectable Hydrogels Using Chemical Exchange Saturation Transfer MRI. ACS Biomater Sci Eng. 2015:227–237.
118. Slaughter MS, Soucy KG, Matheny RG, Lewis BC, Hennick MF, Choi Y, Monreal G, Sobieski MA, Giridharan GA, Koenig SC. Development of an extracellular matrix delivery system for effective intramyocardial injection in ischemic tissue. ASAIO J. 2014:730–736. [PubMed: 25232775]
119. O'Cearbhaill ED, Ng KS, Karp JM. Emerging medical devices for minimally invasive cell therapy. Mayo Clin Proc. 2014:259–273. [PubMed: 24485137]
120. Hastings CL, Roche ET, Ruiz-Hernandez E, Schenke-Layland K, Walsh CJ, Duffy GP. Drug and cell delivery for cardiac regeneration. Adv Drug Deliv Rev. 2015:85–106.
121. Arnal-Pastor M, Monlen JCM, Valls- Lluch A. Regenerative Medicine and Tissue Engineering. InTechOpen, Rijeka, Croatia. 2013
122. Ota T, Patronik NA, Schwartzman D, Riviere CN, Zenati MA. Minimally invasive epicardial injections using a novel semiautonomous robotic device. Circulation. 2008:S115–S120. [PubMed: 18824742]
123. Awada HK, Hwang MP, Wang Y. Towards comprehensive cardiac repair and regeneration after myocardial infarction: Aspects to consider and proteins to deliver. Biomaterials. 2016:94–112.
124. Reis LA, Chiu LL, Feric N, Fu L, Radisic M. Biomaterials in myocardial tissue engineering. J Tissue Eng Regen Med. 2016:11–28. [PubMed: 25066525]

125. Kovacic JC, Fuster V. Cell Therapy For Patients With Acute Myocardial Infarction: ACCRUEd Evidence to Date. Circ Res. 2015:1287–1290. [PubMed: 25858059]

126. Karantalis V, Hare JM. Use of Mesenchymal Stem Cells for Therapy of Cardiac Disease. Circ Res. 2015:1413–1430. [PubMed: 25858066]

127. Matsuura K, Haraguchi Y, Shimizu T, Okano T. Cell sheet transplantation for heart tissue repair. J Control Release. 2013:336–340. [PubMed: 23500057]

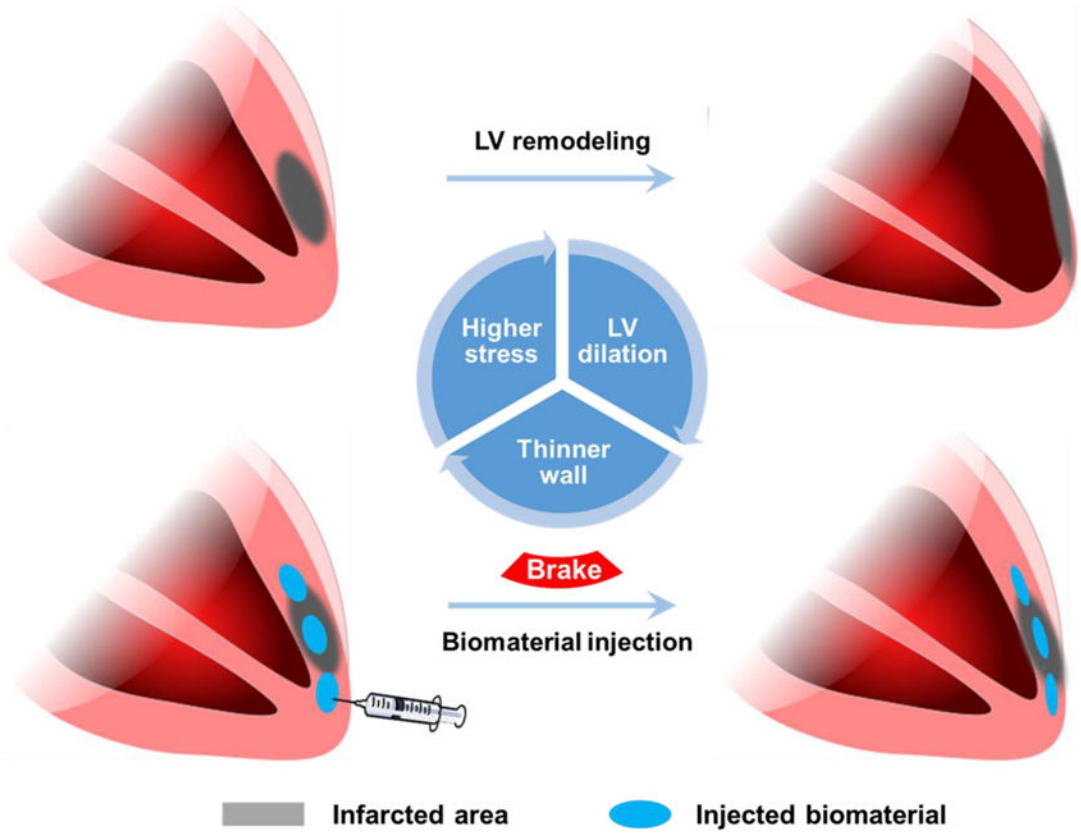

Figure 1.
Left ventricular (LV) remodeling and intramyocardial biomaterial injection therapy. The LV wall thickness is better maintained by biomaterial injection, and lower wall stress is believed to contribute to the preservation of LV geometry.

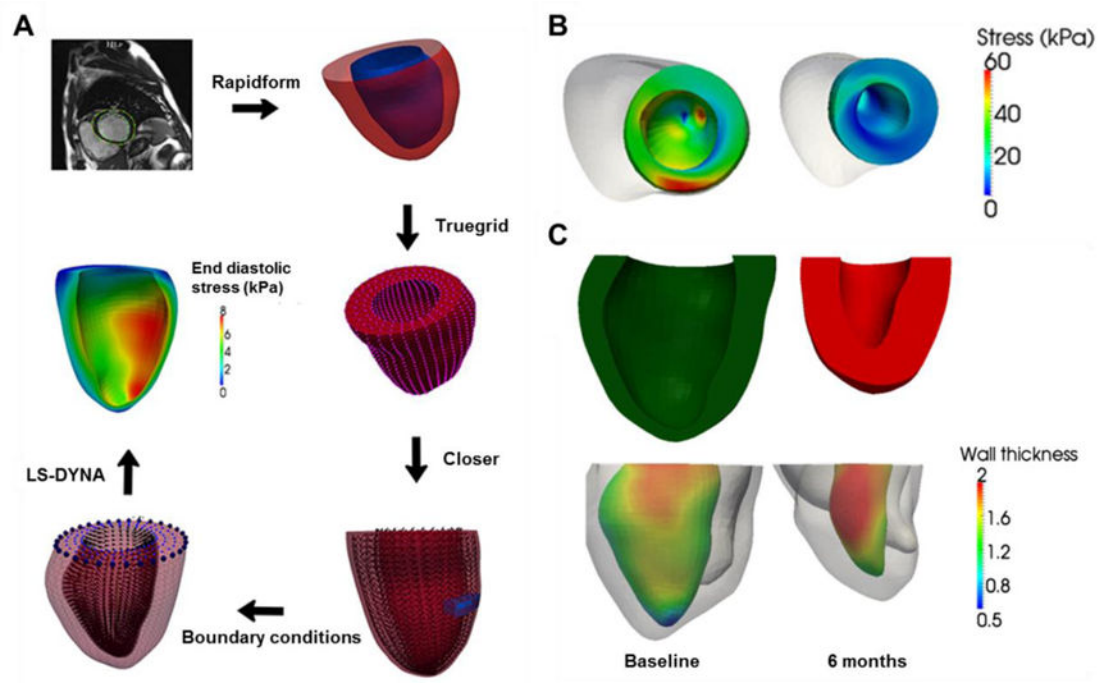

Figure 2.

(A) Process of quantification of left ventricular wall stress from MRI characterization to FE modeling results [20]. Rapidform, Truegrid, Closer and LS-DYNA are software routines implemented to achieve the next step. (B) Calculated end-systolic regional myofiber stress distribution at baseline (left) and 6 months after injection (right) in a patient [21]. (C) Top: LV cross-section view at baseline (left) and 6 months (right). Bottom: regional LV wall thickness measured based on the MRI-reconstructed LV geometry of the same patient in (B) [21]. Wall thickness unit: cm.

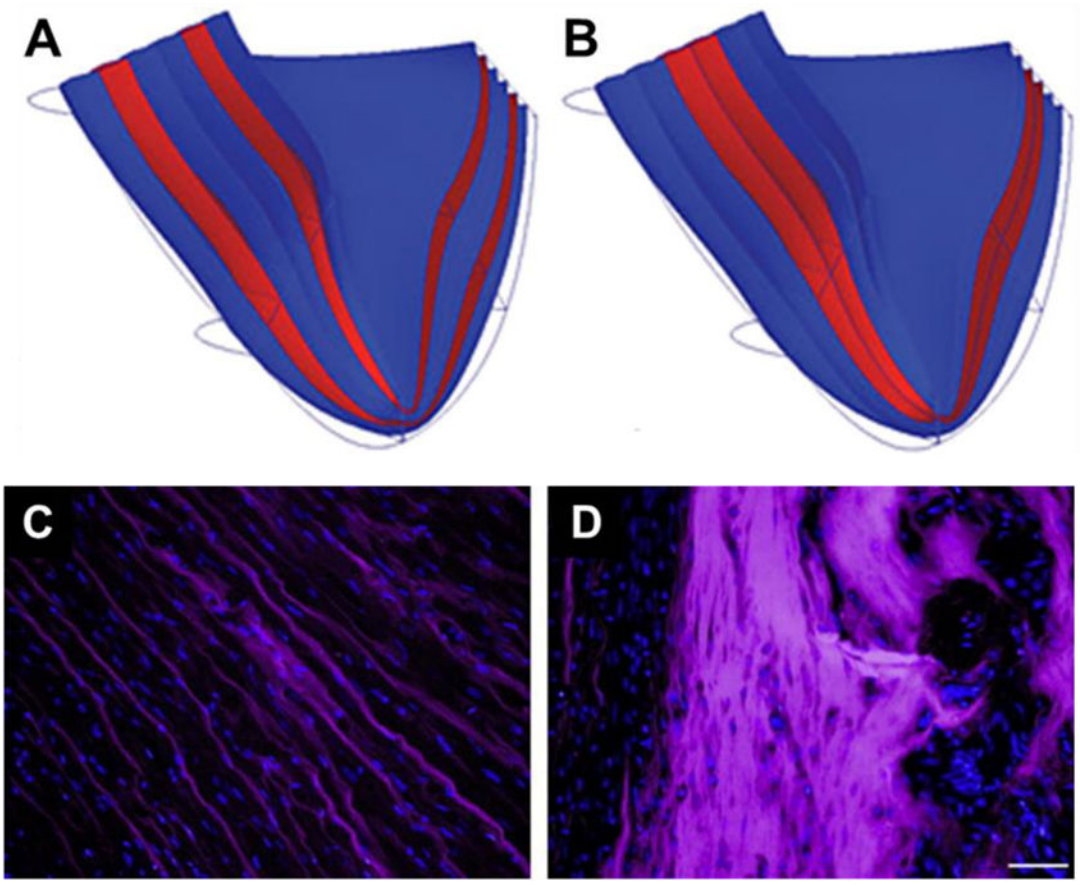

Figure 3.

Biomaterial distribution in silico and in vivo. (A,B) Cross-section of infarcted heart with different injectate distributions in an FE model [54]: (A) layered injectate in infarcted LV represented as transmural layers (red); (B) bulk injectate in infarcted LV represented as transmural layers (red). (C,D) Alexa Fluor 660 labelled PEG hydrogel (purple) distribution in infarcted rat hearts 30 min after injection [55]. Hydrogel injected (C) immediately after infarction, and (D) 7 days after infarction. Scale bar = 50 μm for C and D.

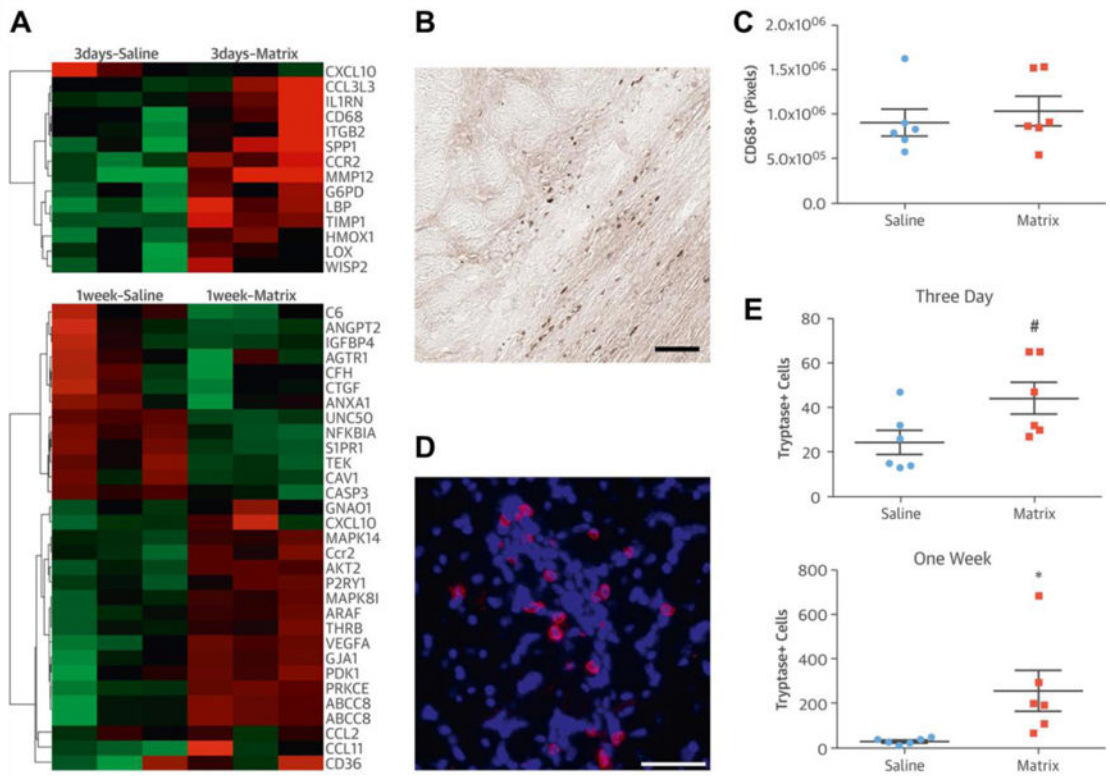

Figure 4.

(A) Expression of inflammation related genes (red = upregulated; green = downregulated) at 3 d and 1 w after injection. (B) $CD68^+$ macrophages (brown) in a myocardial ECM-injected infarct 3 d after injection. (C) Quantification of $CD68^+$ macrophages in the infarcted LV wall 3 d after injection. (D) $Tryptase^+$ (red) cells in myocardial ECM injected heart 1 w after injection; nuclei (blue). (E) Quantification of $tryptase^+$ mast cells in the infarcted LV wall 3 d and 1 w after injection. Scale bars = 50 μm. #$p = 0.052$. *$p < 0.05$. [68]

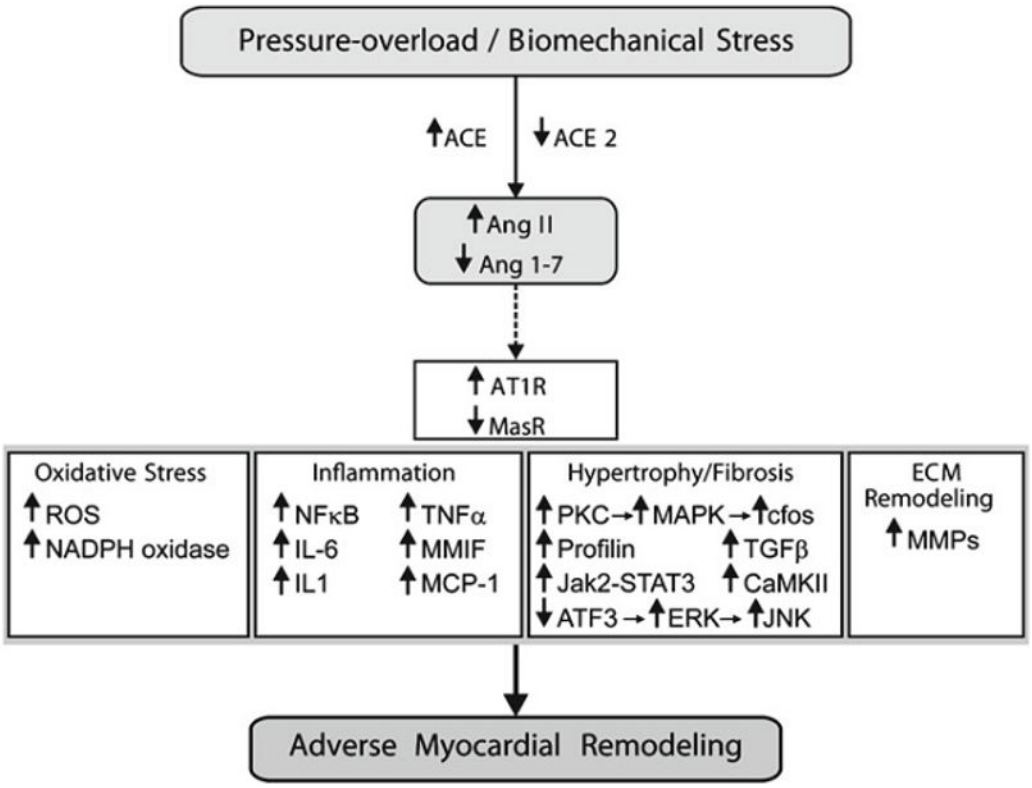

Figure 5.

Role of Ang II signaling in adverse myocardial remodeling. Solid connecting arrows = enzymatic pathway; broken arrows = peptide agonist interacting with its key receptor; Bold arrow = stimulatory effect. ACE: angiotensin-converting enzyme; AT1R: Ang II type 1 receptor; ATF3: Activating transcription factor 3; CaMKII: $Ca2^{+}$/calmodulin-dependent protein kinases II; ERK: extracellular signal-regulated kinase; IL-6: interleukin-6; JAK2-STAT: Janus Kinase 2-signal transducer and activator of transcription system; JNK: C-jun-N-terminal kinase; MAPK: mitogen-activated protein kinase; MasR: Ang 1–7 receptor; MCP-1: monocyte chemoattractant protein 1; MMIF: macrophage migration inhibitory factor; MMP: matrix metalloproteinase; NADPH: nicotinamide adenine dinucleotide phosphate; NFκB: nuclear factor kappa-light-chain-enhancer of activated B cells; PKC: protein kinase C; ROS: reactive oxygen species; TGF-β1: transforming growth factor-β1; TNF-α: tumor necrosis factor-α [59].

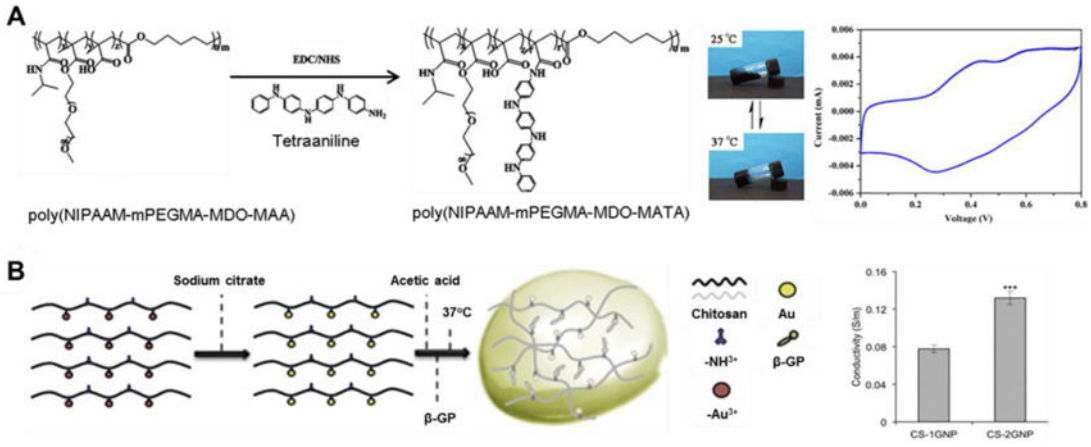

Figure 6.

Examples of conductive injectable biomaterials. (A) Synthesis of electroactive tetraaniline-containing thermosensitive (PN-TA) hydrogels and cyclic voltamogram of a PN-TA copolymer. mPEGMA: methoxy(polyethylene glycol) methacrylate; MDO: 2-methylene-1,3-dioxepane; MAA: methacrylic acid [81]. (B) Preparation of conductive gold nanoparticle-chitosan thermosensitive (CS-GNP) hydrogels; four-point probe conductivity of CS hydrogel with different concentrations of gold nanoparticles (n = 3, ***$p < 0.001$). β-GP: β-glycerophosphate disodium salt [82].

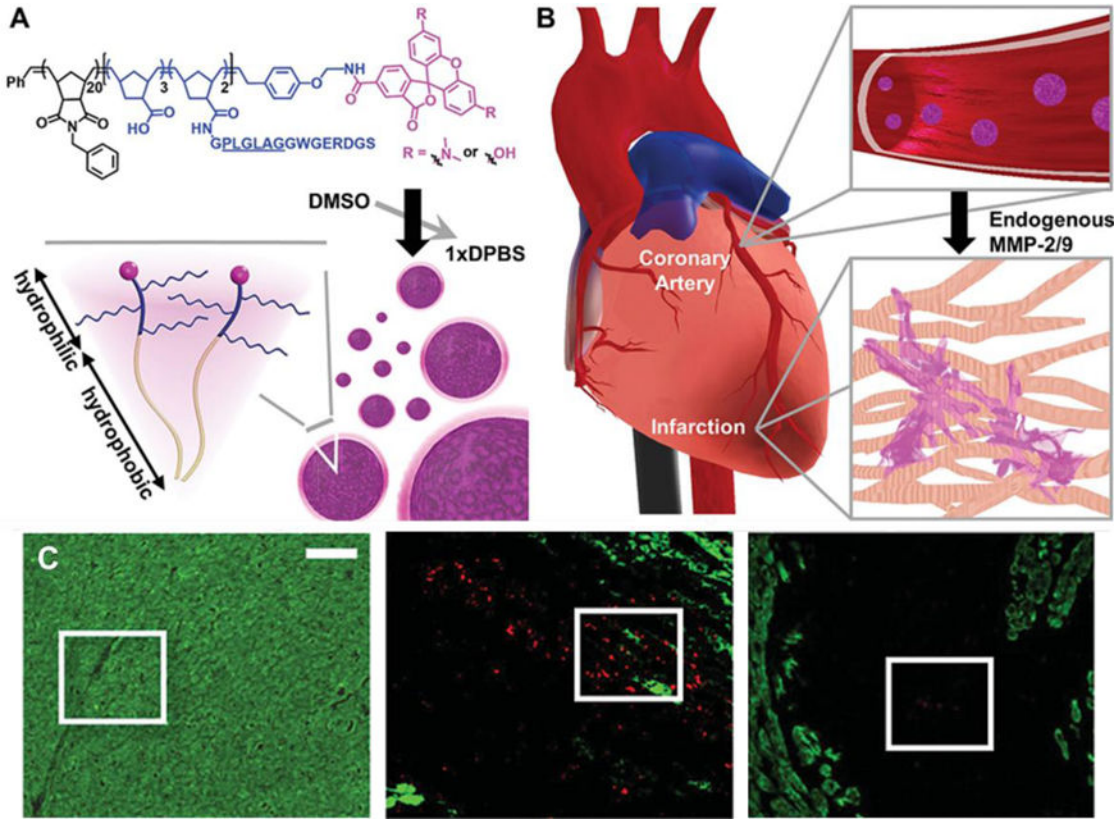

Figure 7.

(A) Peptide-polymer amphiphile (PPA) containing an MMP-2 and MMP-9 specific recognition sequence (underlined), and PPA nanoparticles self-assembled through hydrophobic-hydrophilic interactions when dialyzed into aqueous buffer. (B) Circulating nanoparticles in the bloodstream (not to scale) upon intravenous delivery. (C) Retention of intravenously delivered nanoparticles in the myocardium. Red: Labeled PPA 2 d post-injection, green: α-actinin. Areas within white boxes are enlarged in the original publication and show retention of PPA nanoparticles in these areas. Scale bar = 50 μm [93].

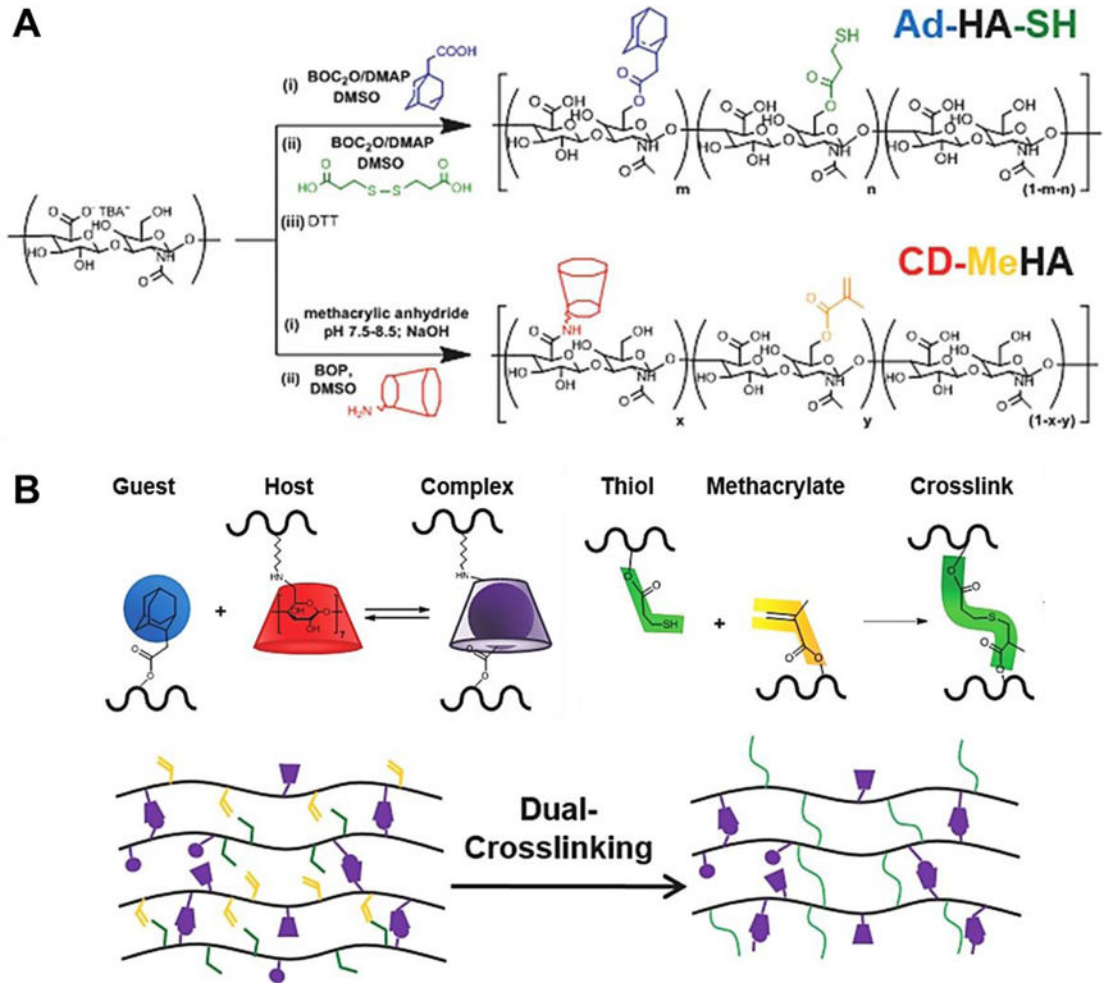

Figure 8.

Synthesis of guest Michael-donor (Ad-HA-SH, Ad: adamantine) and host Michael-acceptor (CD-MeHA, CD: β-cyclodextrin, MeHA: methacrylated HA) macromers. (B) Schematic of dual-crosslinking hydrogel formation: interaction of Ad (guest) and CD (host) in formation of a reversible guest-host complex crosslink; addition of thiol and methacrylate in formation of a covalent crosslink [96].

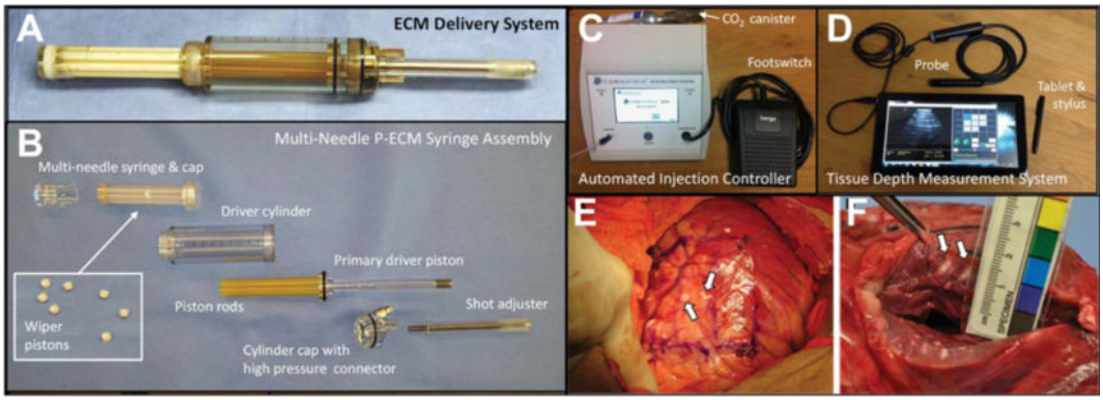

Figure 9.

ECM delivery system components and intramyocardial ECM injection. (A) Assembled ECM delivery system loaded with ECM. (B) Components of disassembled ECM delivery system: multi-needle ECM syringe and wiper pistons (inset). (C) Automated injection controller with a pneumatic footswitch pedal and a disposable CO_2 canister. (D) Tissue depth measurement system including tablet for real-time cardiac imaging guided delivery of ECM. (E) In vivo ECM injection sites (white arrows) in bovine LV lateral wall epicardium. (F) Close-up view of measuring ECM material penetration distance [118].

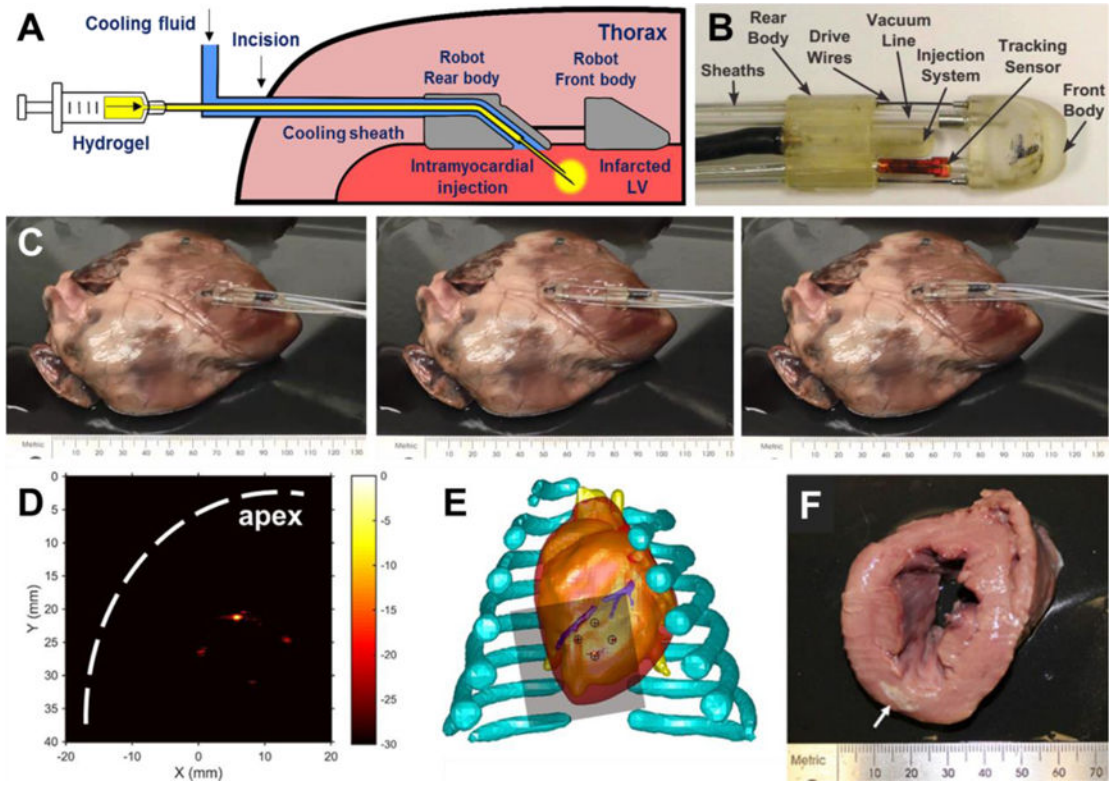

Figure 10.

Subxiphoid transepicardial injection of thermoresponsive hydrogel for myocardial injection therapy. (A,B) Components of the modified HeartLander with cooling feature and illustration of transepicardial hydrogel injection. (C) Ex vivo demonstration of HeartLander crawler moving on porcine heart through “release-approach-anchor” cycles. (D) Photoacoustic imaging of patterned injections made in a beating porcine heart. The signals of injected hydrogel away from apex were weaker due to energy loss through tissue. (E) Match between pattern of injected hydrogel with planned injection sites. (F) Injected hydrogel in LV myocardium (arrow: hydrogel) [107].

Table 1

Summary of recent large animal studies of intramyocardial biomaterial injection therapy.

Material	Species	MI Model	Injection time	Injection volume	Observation time	Cardiac function	Reference
Modified HA	Yorkshire pigs, 65–70 kg	Permanent ligation of proximal LCx	60 min after	30 × 200 μL	8 weeks	Improved EF, FAC	31
Modified HA	Yorkshire pigs, 25 kg	Permanent ligation of OM1 and OM2	Immediately after	9 × 100 μL	2 weeks	No functional improvement	32
Modified HA	Yorkshire pigs, 40–50 kg	Permanent ligation of LCx and OM branches	30 min after	20 × 300 μL	12 weeks	Improved EF, ESV	33
Modified HA	Dorset sheep, 35–40 kg	Permanent ligation of the LAD and DB	30 min after	20 × 300 μL	8 weeks	No improvements in EF, only one hydrogel group improved ESV	34
Modified HA	Dorset sheep, 45 kg	Permanent ligation of OM branches	30 min after	16 × 300 μL	8 weeks	Improved EF, ESV	35
Calcium hydroxyapatite microspheres	Sheep, 35–40 kg	Permanent ligation of LAD and DB	Within 3 h	20 × 130 μL	8 weeks	Improved EF, greater infarct blood flow	36
Calcium hydroxyapatite microspheres	Yorkshire pigs, 37.2 ± 1.2 kg	Permanent ligation of LCx or its branches	30 min after	20 × 150 μL	4 weeks	Improved EF, ESV, EDV	37
Calcium hydroxyapatite microspheres	Yorkshire pigs, 25 kg	Permanent ligation of OM1 and OM2	Immediately after	20 × 150 μL	3 weeks	Improved EF	38
Calcium hydroxyapatite microspheres	Sheep, 35–40 kg	Permanent ligation of LAD and DB	Within 60 min	1.3 mL (n=6) or 2.6 mL (n=5)	8 weeks	EDV decreased with 2.6 mL injection but not with 1.3 mL	39
VentriGel (ECM)	Yucatan mini pigs. 45–50 kg	Percutaneous coil embolism infarct of LAD	2 weeks after	14 to 15 × 250 μL	3 months	Improved EF, FAC	30
VentriGel (ECM)	Yucatan mini pigs, 28–40 kg	Percutaneous coil embolism infarct of LAD	2 weeks after	15 × 250 μL	1–2 h	Not reported	29
Particulate ECM	Jersey calves, 65–95 kg	Polystyrene latex microspheres embolization of LAD and/or LCx	30 days after	9–11 mL	60 and 90 days	Improved EDP, ESV, EDV; n=2 for each group	42
Algisyl-LVR (Alginate)	Canine	Polystyrene latex microspheres embolization of LAD and LCx	2 weeks after	7 injections, total 1.8 to 2.1 mL	17 weeks	Improved EF, ESV, EDV	17
Modified PEG	Goat, 70 kg	75 min occlusion of proximal LCx	4 weeks after	10 × 200 μL	4 weeks	Not reported	40
PDGF binding peptide	Mini pigs, 5 months old	Permanent occlusion of LAD	Immediately after	40 × 50 μL	12 weeks	Improved EDP and -dP/dt	41

LAD: left anterior descending artery; LCx: left circumflex artery; OM: obtuse marginal artery; DB: diagonal branches; PEG: polyethylene glycol; PDGF: platelet-derived growth factor.